PROMOTION OF IN VIVO 5-AMINOLEVULINIC ACID-PHOTODYNAMIC THERAPY EFFICACY BY MEK INHIBITION

By Jayoti Som

A thesis submitted to the School of Graduate Studies in partial fulfillment of

the requirements for the degree of

Master of Science in Medicine

(Cancer and Development)

BioMedical Sciences

Faculty of Medicine

October 2020

Memorial University of Newfoundland

St. John's

Newfoundland and Labrador

Abstract

Protoporphyrin IX (PpIX), a heme precursor, is a photosensitizer that is selectively accumulated in cancer cells when pretreated with its precursor, 5-aminolevulinic acid (5-ALA). Exposure of PpIX accumulating-cancer cells to red light induces the generation of reactive oxygen species (ROS) and subsequent stimulation of cancer cell death, which is known as 5-ALA-photodynamic therapy (5-ALA-PDT). Previously, Dr. Hirasawa's lab discovered that inhibiting the oncogenic Ras/MEK pathway increases PpIX accumulation in cancer cells by suppressing PpIX efflux and PpIX conversion to heme. Here, we sought to determine whether the increase of PpIX accumulation by MEK inhibition promotes 5-ALA-PDT efficacy. First, we classified seven human cancer cell lines into three groups – sensitive, moderately sensitive, and least sensitive – based on their sensitivities to 5-ALA-PDT. Pretreating the moderately sensitive and least sensitive cell lines with a MEK inhibitor increased their sensitivities to 5-ALA-PDT, suggesting that MEK activity influences PDT sensitivity of cancer cells. MEK inhibition promoted 5-ALA-PDT induced generation of ROS and the subsequent programmed cell death. Furthermore, combined 5-ALA-PDT with a MEK inhibitor was significantly effective in inhibiting the growth of tumors in nude mice implanted with human colon cancer cells (DLD-1) and increased their overall survival. As the efficacy and safety of MEK inhibitors are clinically established, combined 5-ALA-PDT with MEK inhibition could directly impact 5-ALA-PDT applications in the clinic.

General Summary

Although the advancements in treatment modalities have improved the outcomes in cancer treatment, there is still scope for improvement, and newer and better treatment strategies need to be developed to achieve better patient care. Photodynamic therapy is a cancer treatment strategy that uses special light-activated chemical compounds called photosensitizers. On exposure to light, these photosensitizers generate highly active oxygen moieties that induce cancer cell death. Earlier, research at the Hirasawa Lab discovered that targeting a specific cell signaling pathway, the Ras/MEK pathway, with inhibitors, could improve the accumulation of photosensitizers in the cancer cell. In this study, I sought to determine whether this improved accumulation of photosensitizers would improve treatment efficacy. My results show that different cancer cell lines have different sensitivities to photodynamic therapy. Further, the Ras/MEK inhibition strategy improved the treatment efficacy of photodynamic therapy both in the cells and in mouse models of cancer. These are significant preclinical results that show that the Ras/MEK inhibition strategy could be utilized to improve the treatment outcome of photodynamic therapy of cancer in the clinic.

Co-authorship Statement

In this thesis, all *in vitro* experiments were performed by the author, Jayoti Som. The animal studies were performed as a group, which included Jayoti Som, Suzette Rutihinda, and Vipin Shankar.

Results from this thesis were published in the British Journal of Cancer under the title “Systemic MEK inhibition enhances the efficacy of 5-aminolevulinic acid-photodynamic therapy,” (Br J Cancer . 2019 Oct;121(9):758-767. doi: 10.1038/s41416-019-0586-3. Epub 2019 Sep 25). This is an open access article, under creative common license.

Acknowledgments

I would like to thank my supervisor Dr. Kensuke Hirasawa, my mentors Dr. Vipin Shankar Chellakot, and Dr. Maria Licursi, and all my colleagues for helping me tremendously during my research. I would like to extend my gratitude to my committee members Dr. Ann Dorward and Dr. Edward Kendell, for guiding me throughout the degree. I would also like to thank the Canadian Cancer Society, Memorial University of Newfoundland, and all other Funding Agencies for their generous contribution. Lastly, I would like to thank my family and friends for supporting me throughout the degree.

Table of Contents

List of Figures

List of Tables

List of Abbreviations

5-ALA	5-Aminolevulinic Acid
ABC transporter	ATP-binding cassette transporter
ATCC	American Type Culture Collection
CCVK	Colorimetric cell viability kit
DMEM	Dulbecco's modified Eagle's medium
DMSO	Dimethyl sulfoxide
DW	Distilled water
EMEA	European Medicine Evaluation Agency
ERK	Extracellular signal-regulated kinase
FBS	Fetal bovine serum
FDA	Food and Drug Administration
FECH	Ferochelatase
MAPK	Mitogen-activated protein kinase
MEK	Mitogen-activated protein kinase kinase
MNK	MAP kinase-interacting serine/threonine-protein kinase
NSCLC	Non-small cell lung cancer

PI3K	Phosphoinositide 3-kinase
P38 MAPK	P38 mitogen-activated protein kinase kinase
PBS	Phosphate-buffered saline
PDX	Patient-derived xenograft
PDD	Photodynamic Diagnosis
PDT	Photodynamic Therapy
PpIX	Protoporphyrin IX
PS	Photosensitizer
RIPA	Radioimmunoprecipitation assay
ROS	Reactive Oxygen Species
RSK	ribosomal s6 kinase (rsk)
WHO	World Health Organization

Chapter 1. Introduction

1.1. Cancer incidence and currently available treatment strategies

According to the World Health Organization (WHO), cancer is the second leading cause of death, and almost 8.8 million people died from cancer in 2015 globally (*WHO, Key Facts about Cancer*, 2014). In the United States, 1,735,350 people were diagnosed with cancer in 2018, and $147.3 billion was spent on cancer care in 2017 (*Cancer Statistics Review, 1975-2016 - SEER Statistics*, 2020). The overall rate of cancer mortality is declining globally; as of 2015, the cancer death rate decreased by 26% since its peak from the 1990s owing to advanced treatment modalities and facilities, early detections, and reduced smoking (Siegel *et al*., 2018). Surgery, chemotherapy, radiotherapy, immune therapy, and combination therapy are the current cancer treatment options. The treatment modality is decided based on the cancer type, disease stage and advancement, and the age and background of the patient.

Surgery is the primary therapeutic option for many solid tumors (Klepper, 2016). However, surgery has many limitations, such as failure to remove tumors from inoperable areas, inability to achieve complete removal of tumors and to distinguish between normal tissue and tumors, and damaging healthy tissues leading to decreased quality of life (4). Surgery is also often associated with many complications, such as increased risks of infections and prolonged recovery time.

All the systemic therapies (chemotherapy, immune therapy, hormone therapy, targeted therapy) use a single or combination of drugs that target the cancer cells and destroy them locally or throughout the body. Drug therapies are often repeated, and every cycle of treatment is usually followed by a period for recovery. The selection of the drugs and number of cycles of treatment

mainly depends on the type and stage of cancer, and age, and overall health of the patient (Atkins & He, 2019; Pinedo & Giaccone, 1997)

Chemotherapy drugs, often referred to as "chemo drugs," target actively growing cells such as cancer cells by arresting their cell cycles. The main advantage of chemo drugs is that they circulate throughout the patient's body, and hence can be effective for metastasized cancers. Traditional chemo drugs could be used before surgery to decrease the size of the tumor, or after surgery to prevent cancer recurrences. A combination of multiple chemo drugs often achieves the best results (Raguz & Yagüe, 2008). Though traditional chemotherapy drugs are very effective in treating cancer, they often cause significant side effects on the body. While attacking highly proliferating cancer cells, chemo drugs also damage normal cells with rapid cell division, such as hair follicles, the lining of the digestive system, and bone marrow cells, which lead to hair loss, gastrointestinal symptoms, and bone marrow degeneration, respectively (Raguz & Yagüe, 2008). Resistance to chemo drugs is one of the biggest challenges in cancer treatments. The heterogeneous nature of cancer cells and the mutations in the cancer cells contribute to the development of resistance to chemo drugs (Gerber, 2008).

Targeted therapies, a recently developed treatment modality, involve monoclonal antibodies or small molecule inhibitors, that can be customized depending on the specific genetic background and cancer type of the individual patient (Gerber, 2008). This therapy interferes with specific molecular components required for tumor growth and progression and does not affect normal cells. Monoclonal antibodies exert anti-cancerous activities by different mechanisms such as binding and neutralizing ligands to disrupt tumor growth, blocking receptor binding sites necessary for tumor growth, or blocking immune-suppressive signaling to activate antitumor

immunity (Scott *et al*., 2012). As of December 2019, 79 therapeutic mAbs have been approved by the United States Food and Drug Administration (US FDA) (Lu *et al*., 2020).

It has been reported that small molecule inhibitors that interfere with cell signaling pathways, such as the tyrosine kinase signaling pathway, are effective for cancer treatment (Gerber, 2008; *Targeted Cancer Therapies Fact Sheet - National Cancer Institute*, 2020). The various tyrosine kinase signaling pathways promote cell growth, proliferation, and angiogenesis and are usually activated in cancers. Targeting these pathways with small molecule inhibitors is an economical and effective strategy for cancer treatment. Further, the small molecule inhibitors could be designed to target multiple proteins and signaling pathways, and could hence be more effective compared to monoclonal antibodies (*Targeted Cancer Therapies Fact Sheet - National Cancer Institute*, 2020). However, targeted therapy drugs can cause side effects different from those induced by chemo drugs, such as diarrhea, liver problems, high blood pressure, skin rashes, and blood clotting. These side effects, however, are easily tolerated, and therefore cancer therapies with small molecule inhibitors are considered less toxic compared to chemotherapy drugs. Nevertheless, it is challenging to find the right dosage of small molecule inhibitors for effective treatments (Gerber, 2008; *Targeted Cancer Therapies Fact Sheet - National Cancer Institute*, 2020). Additionally, the treatment outcome is highly patient-dependent.

Radiotherapy uses high energy radiation to damage the DNA of cancer cells extensively, slowing down tumor growth or killing tumors (*Radiation Therapy for Cancer - National Cancer Institute*, 2020; The American Cancer Society Medical and Editorial Content Team, 2018). Two types of radiation therapy are used to treat cancer – external beam and internal beam. The radiation therapy with an external beam involves a machine emitting the radiation, specifically on the tumor site. In contrast, radiation therapy with an internal beam involves a liquid or solid radiation

source that is placed within the body. Internal radiation therapy with a liquid radiation source is given through an injection, swallowing as a capsule, or IV channel, which travels through the bloodstream. While killing cancer cells, radiation can also damage healthy tissues. The side effects depend on the area of treatment and include fatigue, exhaustion, diarrhea, hair loss, skin problems, and increased risk of developing other cancers (*Radiation Therapy for Cancer - National Cancer Institute*, 2020; The American Cancer Society Medical and Editorial Content Team, 2018).

Immunotherapy activates the patient's immune system to fight against tumors. Different types of immunotherapies are currently used to treat cancer, including monoclonal antibodies that specifically target cancer cells, immune checkpoint inhibitors that increase recognition of cancer cells by the immune system, cancer vaccines that boost cancer immunity, and adoptive cell transfers that activate antitumor cytotoxic T cells (American Cancer Society, 2015; National Cancer Institute, 2019). The dosage and duration of immunotherapy depend on the type and stage of cancer. Although immunotherapy is not as common as surgery or chemotherapy, it has been approved for the treatment of many cancers. The common side effects of immunotherapy are pain, rash, itching, swelling, redness, diarrhea, blood pressure changes, trouble breathing, and heart palpitations (American Cancer Society, 2015).

Although chemotherapy and radiotherapy are widely used in clinics, surgery remains the primary treatment for solid tumors. As surgery without substantial damage to the healthy tissues is very critical, new cancer treatments such as photodynamic therapy (PDT) are essential to be established.

1.2. Photodynamic Therapy (PDT)

PDT is an FDA approved, drug-device combination for cancer treatment. It involves the use of photosensitizers (PS), which are chemical compounds that are activated when exposed to light. The activated photosensitizer stimulates the conversion of molecular oxygen present in the tissues to highly toxic molecules called reactive oxygen species (ROS). (Agostinis *et al*., 2011) (Fig 1). None of the three components of PDT, PS, light, or molecular oxygen are toxic by themselves, but when they are combined, they generate photo-toxicity and induce cancer cell death. PDT has been approved for the treatment of colon cancer, head and neck cancer, prostate cancer, esophageal cancer, melanoma, actinic keratosis, and non-small cell lung carcinoma (Huang, 2005; Wan & Lin, 2014).

PDT is a two-step process – administration of PS and irradiation of the tumor site with visible light. Owing to the increased metabolic rate and decreased lymphatic drainage in the tumor, the PSs accumulate in the cancer cells (Briel-Pump *et al*., 2018; Kim *et al*., 2011). On exposure to specific wavelengths of light, PSs are activated, inducing the generation of toxic ROS, which oxidizes biomolecules in the cancer cells resulting in cell death. Since the accumulation of the PS is limited to the cancer cells and the tumor tissue, and only the tumor is exposed to light during the treatment, the toxic effects are limited to the tumor, and the surrounding cells are spared. In addition to the direct killing of cancer cells, PDT damages tumor vasculature and initiates inflammatory responses leading to tumor regression (Agostinis *et al*., 2011). Unlike surgery, chemotherapy, and radiotherapy, PDT is less expensive and less invasive and requires short treatment duration. Moreover, PDT does not cause significant pain or side effects (Agostinis *et al*., 2011).

However, similar to other cancer treatments, PDT also has some limitations. Failure to accumulate a sufficient amount of the PS in the tumor could result in a partial or incomplete treatment outcome. Hyper-photosensitivity is another challenge for many patients, which can cause skin burns, rashes, and pain. Most importantly, the treatment efficacy is dependent on the adequate illumination of the tumor. Since the penetration potential of light is limited to about 1 cm into the human tissue, sufficient illumination of large, deep, and metastasized tumors is often challenging (Agostinis *et al*., 2011).

Fig 1: The three components of photodynamic therapy (PDT). PDT involves the use of a photosensitizer (PS), which gets accumulated in cancer cells. On irradiation with light of specific wavelengths, the photosensitizer induces the generation of reactive oxygen species, which elicit photo-toxicity and oxidize the cellular components, resulting in cell death.

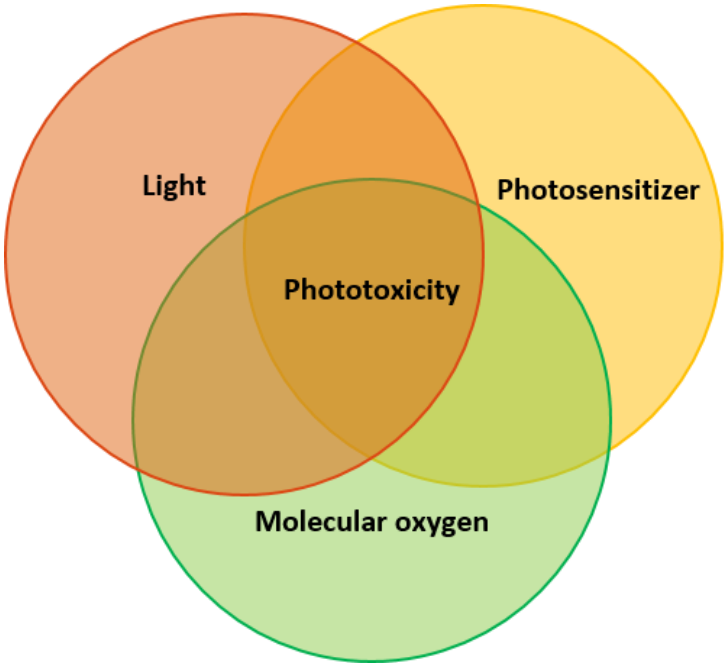
Light
Photosensitizer
Phototoxicity
Molecular oxygen

1.3. The three components for PDT

1.3.1. Photosensitizers (PS)

PSs are molecules that can be activated by light. Many PSs possess a tetrapyrrole structure similar to heme in hemoglobin and usually have an absorption maximum between 600 nm and 800 nm (Castano *et al*., 2004a). An ideal PS should not show any dark toxicity; that is, they should not be toxic in the absence of light, and should be rapidly cleared from the body (Agostinis *et al*., 2011). Light exposure activates the PSs and induces the generation of singlet oxygen ($^1O_2$) or superoxide (O_2^-), which, in turn, induce cancer cell death (Huang, 2005).

Many of the current approved PSs belongs to the porphyrin family (Table 1). Photofrin is the first FDA approved PS for cancer treatment (Huang, 2005). 5-Aminolevulinic Acid (5-ALA), the precursor of protoporphyrin IX (PpIX), is one of the widely used PSs in PDT. PSs can be given directly for tumor cell accumulation. However, some PSs are administered as a prodrug, which is then metabolically converted to the active PS, to avoid intrinsic PS sensitivity (Sansaloni-Pastor *et al*., 2019). 5-ALA is a prodrug, which does not have any fluorescence property. Once administered, it gets metabolically converted to the active PS, protoporphyrin IX (PpIX), through the heme biosynthesis pathway. European Medicine Evaluation Agency (EMEA) approved ALA esters and derivatives for papillary bladder cancer (Casas *et al*., 2009; Krammer & Verwanger, 2009).

Table 1: Photosensitizers (PSs) approved for cancer therapy

Photosensitizer	Structure	Peak absorption (nm)	Approved clinical indications	Reference
Photofrin (Porfimer Sodium)	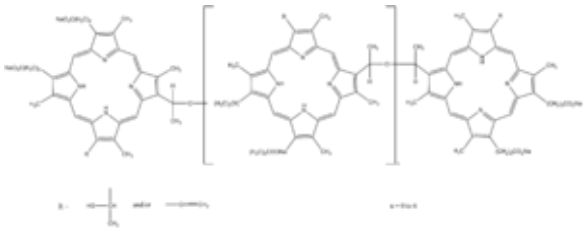	630	Cancers of the Bladder, Brain, Lung, Esophagus, and Bile duct	(Huang, 2005)
5-Aminolevulinic acid	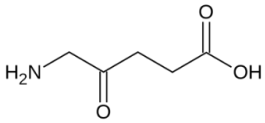	635	Cancers of Colon, Brain, Skin, Bladder, and Esophagus	Wachowska *et al*., 2011)
Verteporfin	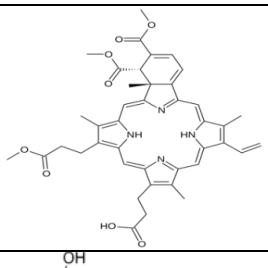	690	Abnormal blood vessels, Pathologic myopia	(Huang, 2005)
Foscan	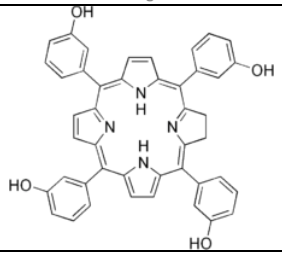	630	Head and neck squamous cell carcinoma	(Huang, 2005)

Fig 2: Schematic diagram of PDT on cancer cells and normal cells. The photosensitizers get selectively accumulated in cancer cells. On exposure to light of specific wavelengths, the PSs get activated and induce the generation of ROS, leading to cell death. However, the PSs do not accumulate in the normal cells, sparing them from cell death.

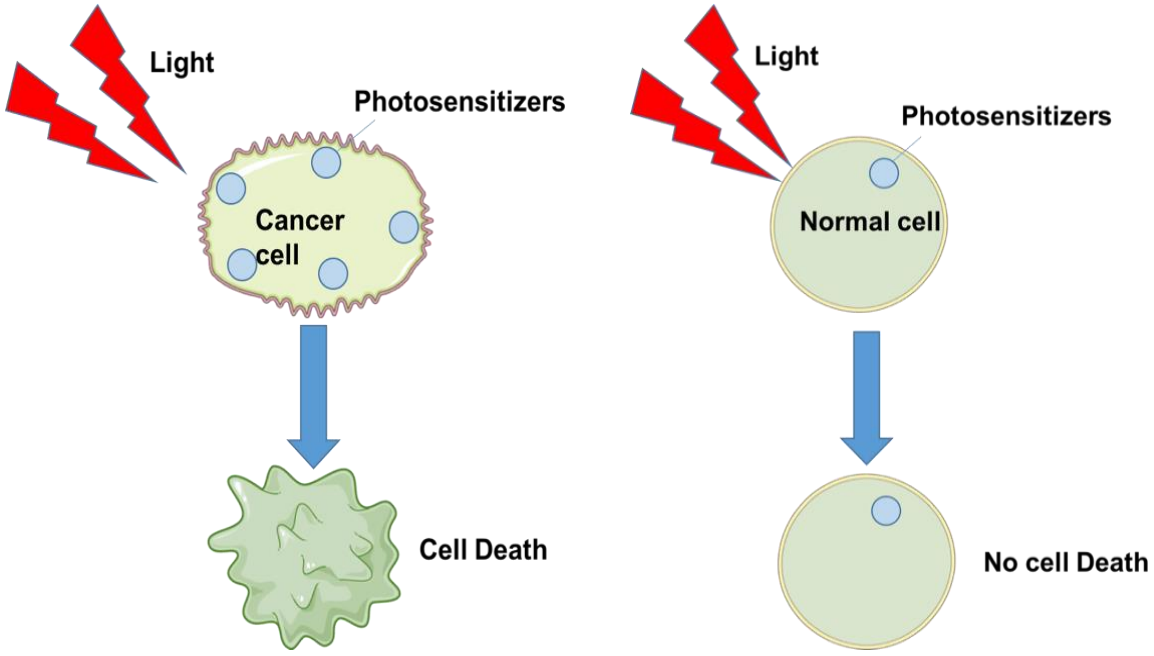
Light
Photosensitizers
Cancer cell
Cell Death
Light
Photosensitizers
Normal cell
No cell Death

1.3.2. Light and light sources

The activation of the PS is dependent on adequate light exposure. Most PSs can be activated by light in the visible spectrum (400 – 600 nm). Although lower wavelength lights have higher energy and can efficiently activate the PSs, they lack sufficient tissue-penetration potential. Red light (~600 nm) has the highest penetration ability, whereas blue light (~400 nm) has the least. Light sources up to a wavelength of 800 nm (far red) have enough energy to generate singlet oxygen ($^1O_2$) in cells accumulated with PSs. Therefore, most PDT applications prefer light in the range of 600 – 800 nm for attaining maximum tissue-penetration.

The light source is chosen based on the size, grade, type, and location of the tumor, and the type of PS. Noncoherent light sources (regular arc lamps) were the first light sources used in PDT. They were affordable, safe, and easy to use. However, they had many disadvantages, such as lack of energy control, high thermal effects on the subject, and significantly low light intensities. Therefore, lasers are currently used as light sources in PDT. These light sources can deliver light of specific wavelengths at high energy intensities to the tumor for effective activation of the PSs (Huang, 2005).

1.3.3. Oxygen

The third element of PDT is molecular oxygen. Sufficient oxygen is required for the effective generation of ROS, which subsequently oxidizes the cells and kills them. It has been shown that the lack of sufficient molecular oxygen (hypoxia) could affect the treatment outcome of PDT (Huang, 2005).

While the unstimulated PSs exist in the ground state (0PS), they are rapidly activated to an excited state (1PS) when exposed to light of sufficient energy. Fig 3 is adapted from the Jablonski Diagram, which shows the fate of the excited PS. From the excited state, PSs can take two different pathways to return to the ground state (Fig 3). First, they can release energy by emitting heat and fluorescence. Alternatively, they move to a triplet state (3PS) by intersystem crossing. As it returns to the ground state, it releases energy, which is transferred to oxygen to generate reactive oxygen species (ROS), such as singlet oxygen and free radicals. These ROS mediate cellular toxicity. The activated sensitizer can undergo two kinds of reactions. First, it can react directly either with the substrate, such as the cell membrane or a molecule, transferring a hydrogen atom to form radicals. The radicals interact with oxygen to produce oxygenated products (type I reaction). Alternatively, the activated sensitizer can transfer its energy directly to oxygen, to form singlet oxygen — a highly reactive oxygen species. These species oxidize various substrates (type II reaction). The ROS thus generated oxidizes cellular components resulting in cell death (Huang, 2005; *Jablonski Diagram - Wikipedia*, 2020; Jabłoństski, 1933).

Fig 3: Jablonski Diagram: A schematic representation of PSs activation and generation of reactive oxygen species. The PS in its ground state (S_0) is readily excited by light to an excited state (S_1). From the excited state, the PS returns to the ground state by releasing energy in the form of heat or light (fluorescence) or undergoes intersystem crossing to attain a triplet state (T_1). The PS in the triplet state then releases electrons either to molecular oxygen (type I reaction) or to other biomolecules (type II reaction) to generate highly toxic reactive oxygen species (ROS) that can trigger cell death.

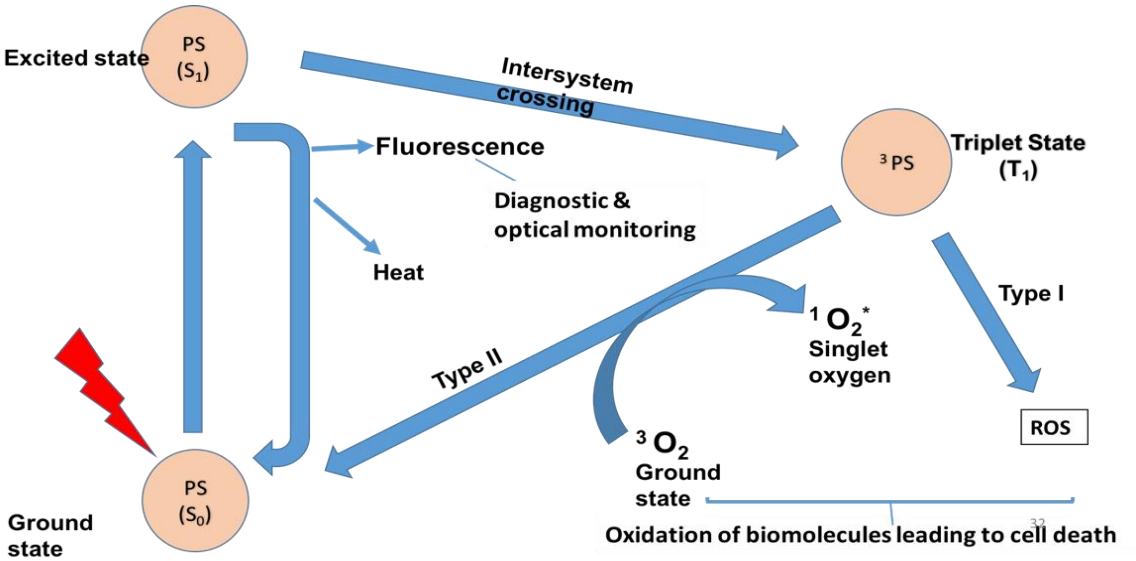
Excited state
PS
(S1)
Intersystem
crossing
Fluorescence
Diagnostic &
optical monitoring
Heat
3 PS
Triplet State
(T1)
Type I
1 O2*
Singlet
oxygen
Type II
ROS
3 O2
Ground
state
PS
(S0)
Ground
state
Oxidation of biomolecules leading to cell death

1.4. Protoporphyrin IX (PpIX)

5-ALA is a precursor of heme in the heme biosynthesis pathway (Ishizuka *et al*., 2011). It is metabolically converted to protoporphyrin IX (PpIX) through several enzymatic processes (Fig 4). The PpIX produced in the cells can either be converted to heme by the enzyme ferrochelatase, or effluxed out of the cell into extracellular space through the ATP-binding cassette (ABC) transporters such as ABCB1, ABCG2, or ABCB6. The heme biosynthesis pathway in a normal cell is highly regulated. The synthesis of 5-ALA and the conversion of PpIX to heme are rate-limiting steps in the pathway. In addition, the rate of ALA synthesis is regulated by the heme concentration in the cell. Higher amounts of heme act as a suppressor of ALA synthesis.

However, in a cancer cell, the pathway is dysregulated, and several steps in between ALA synthesis and the generation of PpIX are overactivated. However, the final enzyme in the pathway, FECH, is downregulated in several cancers. Administration of exogenous 5-ALA by-passes the negative regulation on ALA synthesis and results in increased flux through the pathway. However, due to the downregulation of FECH, the synthesized PpIX is not efficiently converted to heme, resulting in PpIX accumulation in the cancer cells (Ishizuka *et al*., 2011).

PpIX is a photoactive compound and can be excited by visible light. Exposure to red or blue light activates PpIX, inducing the generation of ROS, which oxidizes different biomolecules in cancer cells resulting in cell death. Under blue light, PpIX emits red fluorescence that can be used for tumor detection. This is known as photodynamic diagnosis (PDD) (Fig. 4).

Fig 4: The heme biosynthesis pathway and the use of 5-ALA for photo-diagnosis and photodynamic therapy of cancer. 5-ALA is synthesized in the mitochondria by the enzyme ALA synthase by combining one molecule of glycine with one molecule of succinyl CoA. Once synthesized, 5-ALA is transported across the mitochondrial membrane into the cytoplasm, where the enzymes of the heme biosynthesis pathway convert it into coproporphyrinogen III. Coproporphyrinogen III is transported back into the mitochondria, where it gets converted to protoporphyrin and then into protoporphyrin IX (PpIX). Enzyme ferrochelatase (FECH) chelates a ferrous ion to PpIX and converting it into heme. Heme is then transported into the cytoplasm, where it is either used or broken down. The synthesis of 5-ALA (ALA synthase-catalyzed) and the conversion of PpIX to heme (FECH-catalyzed) are rate-limiting steps in the pathway. Further, there is a feedback inhibition loop between heme and the activity of ALA synthase. However, in a cancer cell, when exogenous 5-ALA is administered, the feedback inhibition on ALA synthase is overridden. PpIX gets accumulated owing to the higher activity of the heme biosynthesis enzymes and the reduced activity of FECH in cancer cells. This PpIX emits red fluorescence, when irradiated with blue light, and can be used to distinguish cancer cells from surrounding normal cells (photodynamic diagnosis; PDD). Additionally, irradiating PpIX with blue or red light, induces the generation of reactive oxygen species (ROS), which oxidizes cellular components leading to cell death.

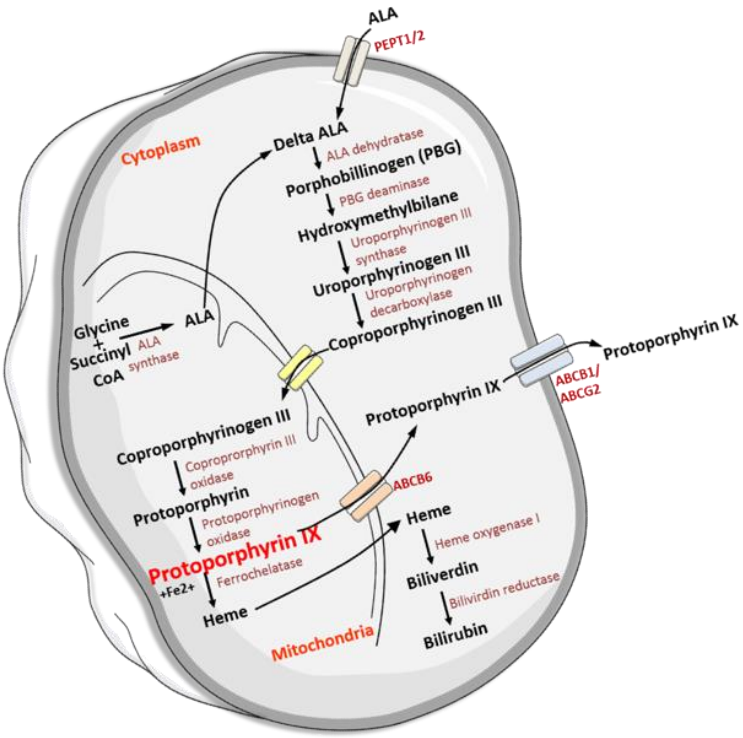
ALA
PEPT1/2
Cytoplasm
Delta ALA
ALA dehydratase
Porphobillinogen (PBG)
PBG deaminase
Hydroxymethylbilane
Uroporphyrinogen III synthase
Uroporphyrinogen III
Uroporphyrinogen decarboxylase
Coproporphyrinogen III
Glycine + Succinyl CoA
ALA synthase
ALA
Protoporphyrin IX
ABCB1/ ABCG2
Coproporphyrinogen III
Coproprorphyrin III oxidase
Protoporphyrin
Protoporphyrinogen oxidase
Protoporphyrin IX
ABCB6
Protoporphyrin IX
+Fe2+
Ferrochelatase
Heme
Heme
Heme oxygenase I
Biliverdin
Biliverdin reductase
Bilirubin
Mitochondria

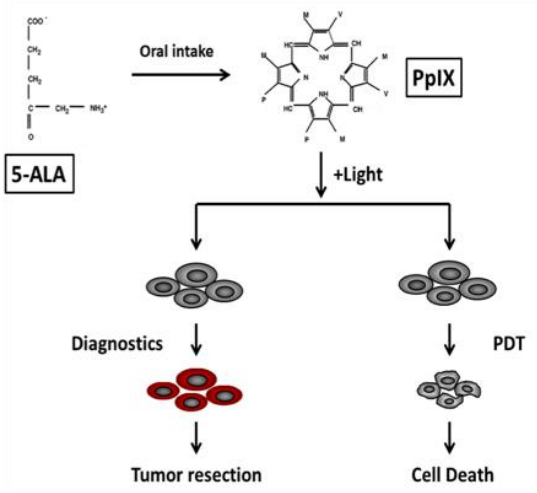
Oral intake
PpIX
5-ALA
+Light
Diagnostics
PDT
Tumor resection
Cell Death

1.5. The Ras/MEK signaling pathway and PpIX accumulation

Ras is a member of a family of proteins that belong to a class of proteins called small GTPases and are involved in transmitting signals within the cells. Ras proteins function as binary molecular switches and control intracellular signaling networks. The Ras-regulated signal pathways control processes such as actin cytoskeletal integrity, cell proliferation, cell differentiation, cell adhesion, apoptosis, and cell migration. Ras and Ras-related proteins are often deregulated in cancers, leading to increased invasion and metastasis, and decreased apoptosis (Khan *et al*., 2019; Shields *et al*., 2000).

The RAS family of proteins were initially identified as Rat Sarcoma factors and is the first oncogene that was identified. The Ras superfamily consists of several members, including Ras, Rab, Rho, Arf, and Ran sub-families. The RAS proteins are monomeric 21-kDa proteins that have a high degree of homology. These proteins function as GTP/GDP-binding signal-transducing molecules from the cell surface to the nucleus.

Ras activates several pathways, of which the mitogen-activated protein kinase (MAPK) cascade has been well-studied (Carriere *et al*., 2008; Friday & Adjei, 2008; Schubbert *et al*., 2007; Weidhaas *et al*., 2006). This cascade transmits signals downstream and results in the transcription of genes involved in cell growth and division. Other Ras-activated signaling pathways are p38 mitogen-activated protein kinase kinase (P38 MAPK) and Phosphoinositide 3-kinase (PI3K) signaling pathways (Yoshioka *et al*., 2018).

MAPK signaling is crucial for maintaining normal physiological processes, including proliferation and differentiation. The MAPK signaling is complex and involves a large number of intermediate molecules, of which the RAS signaling pathway is an important component. The canonical RAS pathway consists of key mediators RAS and RAF along with the intracellular

signal kinases, mitogen extracellular kinase (MEKO, and extracellular signal-related kinase (ERK).

The Ras superfamily members Ras, Rac, Rho, and Cdc42 are involved in the remodeling of the cortical actin cytoskeleton following growth factor stimulation. Ras-GAP, a major regulator of Ras, contains structural domains called the SH3 domains, that are involved in Rho activation and subsequent actin remodeling (Leblanc *et al*., 1998).

The Ras signaling pathways are important regulators of cell proliferation, senescence, and apoptosis. Several Ras downstream effectors have dual roles in each of these processes, such that, under one set of conditions, they promote cell cycle progression and proliferation, while in a different paradigm, they drive cell cycle arrest and apoptosis (Stout *et al*., 2014; Xiang *et al*., 2017). Besides, there are cross talk channels between the Ras downstream effectors that underlies the molecular basis of the intricate control mechanisms that govern cell growth and cell death (Chow *et al*., 2017).

The normal function of the MAPK signaling pathway is to maintain cellular homeostasis. Mutations in the pathway elements lead to signal imbalance and can potentially result in cancer. The Ras/MEK pathway is constitutively activated in many cancers (Datta *et al*., 2017; Santarpia *et al*., 2012; Schubbert *et al*., 2007). Ras activates several downstream cascade branches, including the RAF/MEK/ERK, PI3K/AKT, and RalGDS/Ral signal molecules critical for cancer progression. It has been reported that the interplay between oncogenic Ras and p53, the master tumor suppressor, plays critical roles in the progression of cancer, cellular autophagy, and epithelial-mesenchymal transition (EMT) (X. Zhang *et al*., 2017). Further, this interplay is also reported to regulate the development of chemotherapy resistance and metastasis in several cancers (Janda *et al*., 2002; Liang *et al*., 2019). Based on this evidence, Ras and Ras downstream

effectors, including MAPK and MEK, are considered therapeutic targets for several cancers (Chow *et al*., 2017; Janda *et al*., 2002; Liang *et al*., 2019; Stout *et al*., 2014; X. Zhang *et al*., 2017).

Several previous studies have shown that the activation of oncogenic pathways, including the Ras signaling pathway, increases 5-ALA-induced PpIX accumulation (Juzeniene *et al*., 2007; Li *et al*., 1999; X. Yang *et al*., 2016). Therefore, it was speculated that Ras/MEK activation would increase PpIX accumulation in cancer cells by enhancing the metabolic activities of the heme biosynthesis pathway. However, previous studies at the Hirasawa Lab discovered an opposite effect (Chelakkot *et al*., 2019; Yoshioka *et al*., 2018). They showed that the inhibition of one of the Ras downstream elements, MEK, significantly increases 5-ALA-induced PpIX accumulation in tumors (Yoshioka *et al*., 2018). Further, they demonstrated that MEK inhibition downregulated the expression of ABCB1, a member of ABC transporter, and thus decreased PpIX efflux out of the cells. Additionally, MEK inhibition reduced the activity of FECH, resulting in the low conversion of PpIX to heme (Yoshioka *et al*., 2018). These two independent phenomena together contributed to the enhanced accumulation of PpIX in cancer cells treated with a MEK inhibitor. They concluded that the oncogenic Ras/MEK pathway has a negative effect on 5-ALA-induced PpIX accumulation in cancer cells.

1.6. MEK inhibitors in cancer treatment

MEK1 and MEK2 are key elements in the Ras/MEK pathway and play important roles in regulating angiogenesis, cell proliferation, and cell death. In clinics, MEK inhibitors are widely used as a monotherapy or combination therapy with other cancer treatments (Table 2)

(Sanlorenzo *et al*., 2014). PD98059 is one of the first MEK inhibitors, which inhibits phosphorylation of downstream elements in the Ras/MEK pathway. U0126 inhibits cell proliferation, survival and increases cell death by apoptosis (Hawkins *et al*., 2008). Moreover, U0126 inhibits inflammatory responses by suppressing cytokine production (Yoshioka *et al*., 2018).

Trametinib is the first MEK inhibitor approved by the FDA for the treatment of melanoma (Alexander M Menzies & Long, 2014). In a randomized control trial, Trametinib showed significantly improved treatment outcome and progression-free survival of patients compared to chemotherapy (Alexander M Menzies & Long, 2014). Trametinib is also used with dabrafenib, a BRAF inhibitor in clinics, as a combination for treating metastasized non-small cell lung cancer (NSCLC) (Robert *et al*., 2019). Mutations in the BRAF oncogene are found in several cancers. The most common activating mutation in the BRAF oncogene is a valine substitution for glutamate at residue 600 (V600E) within the BRAF kinase. Although BRAF-targeted therapies are effective in many cancers, inhibiting BRAF activated the downstream MEK, resulting in the development of treatment resistance and disease relapse.

On the other hand, targeting both BRAF and MEK improved the response rate and the treatment outcome (Khunger *et al*., 2018; Robert *et al*., 2019). MEK inhibitor cobimetinib was approved by FDA in 2015 with BRAF inhibitor vemurafenib as a combination drug for the treatment of inoperable or BRAF V600E, or V600K mutated advanced melanoma. Preclinical studies with cobimetinib have demonstrated its ability to inhibit cell division and tumor growth (Cheng *et al*., 2017; Research, 2018). In June 2018, the US FDA and European Medicines Agency (EMA) approved MEK inhibitor Binimetinib with BRAF inhibitor dabrafenib for the treatment of advanced melanoma with BRAFV600 mutation (*National Center for Biotechnology Information,*

PubChem Compound Database, 2018). Binimetinib is a highly selective MEK inhibitor and has the potential to treat many metastasized cancers.

Patients treated with MEK inhibitors sometimes develop mild side effects such as rashes, peripheral edema, diarrhea, and fatigue (Welsh & Corrie, 2015). The MEK inhibitor used in the current study is selumetinib, which is highly selective to inhibit MEK1 and MEK2 (Wu & Park, 2015). Selumetinib has been evaluated in multiple Phase I/II clinical trials. Studies have shown that selumetinib has moderate anti-cancer effects for low-grade gliomas and other cancers, hence not very effective as monotherapy (O'Neil *et al*., 2011). Selumetinib, combined with other chemotherapy such as docetaxel, PI3K inhibitors, carboplatin, and temsirolimus, might be very crucial for successes in clinical trials (Eroglu *et al*., 2015; Van Erp *et al*., 2018).

Table 2: MEK inhibitors approved for clinical use

Inhibitor	Structure	Approved clinical indication	Reference
Trametinib	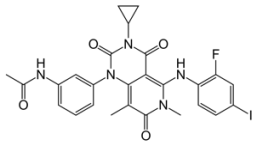	Metastatic melanoma, Non-small cell lung cancer	(*Trametinib - National Cancer Institute*, 2019)
Cobimetinib	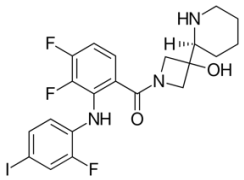	Metastatic melanoma	(A. M. Menzies & Long, 2014)
Binimetinib	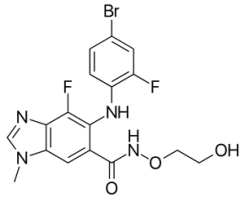	Metastatic tumors with BRAF mutations	(Research, 2018)
PD98059	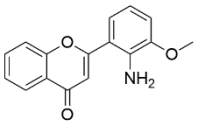	Cervical cancer	(E. J. Yang & Chang, 2011)

Chapter 2. Hypothesis and Study Objectives

2.1 Hypothesis

Based on the previous results from the Hirasawa Lab (Yoshioka *et al*., 2018), which showed that MEK inhibition increases 5-ALA-induced PpIX accumulation, I sought to determine whether increased PpIX accumulation with MEK inhibitor could enhance the sensitivity of cancer cells to 5-ALA-PDT. I hypothesized that the increased PpIX in the cancer cells would induce the generation of higher amounts of ROS and would trigger more extensive cell death. I also hypothesized that combining MEK inhibition with PDT would enhance the efficacy of the treatment.

2.2 Study objectives

To determine the effect of MEK inhibition on the efficacy of 5-ALA-PDT, first, I sought to evaluate the sensitivities of various cancer cell lines to 5-ALA-PDT. Next, the effect of MEK inhibition on 5-ALA-PDT efficacy was determined in the cell lines. Further, animal models of cancers were used to determine the effect of MEK inhibition on 5-ALA-PDT efficacy.

Chapter 3. Materials and Methods

3.1. Cell culture

A panel of cancer cell lines, including colon cancer (DLD-1), lung cancer (H460 & H1299), breast cancer (Hs 578T & MDA-MB-231), and glioma (U118 & U251) were used in the study. Lung cancer (H460 & H1299) cell lines were purchased from American Type Culture Collection (ATCC). Glioma cells (U118 & U251) were obtained from Dr. Tommy Alain (University of Ottawa). The cell lines were authenticated by Short Tandem Repeat (STR) DNA analysis (TCAG Sick kids, Toronto and DDC Medical, USA).

All cell lines were maintained in high glucose Dulbecco's modified Eagle's medium (DMEM) (Invitrogen, Canada). DMEM was supplemented with 10% fetal bovine serum (FBS) (Invitrogen, Canada), sodium pyruvate (Thermo Fisher Scientific, Canada), and antibiotic-antimycotic mixture (Invitrogen Canada) (100 Units/ml penicillin G sodium). The cells were maintained at 37 °C in a humidified atmosphere with 5% CO_2.

3.2 *In vitro* drug treatments

3.2.1. Treatment with MEK inhibitor, U0126

MEK inhibitor U0126 was obtained from Cell Signaling Technology (CST) (Danvers, MA). Five grams of U0126 was dissolved in 500 µl of dimethyl sulfoxide (DMSO) (Sigma, France) to make a 25.97 mM stock solution. The stock solution was stored at -80 °C. Cells were treated with U0126 (20 µM) at 24 h after plating. The controls received an equivalent amount of DMSO.

3.2.2. Treatment with 5-aminolevulinic acid (5-ALA) *in vitro*

5-ALA was obtained from Sigma (Oakville, ON). One gram of 5-ALA was dissolved in 50 ml of DMEM to make a 120 mM stock solution. The stock solution was stored at -20 °C. At 24 h after plating or 20 h after U0126/DMSO treatment, cells were treated with 5-ALA (0.2 mM, 1 mM, 5 mM) and then incubated for 4 h in the dark.

3.3. *In vivo* drug treatments

3.3.1. Administration of MEK inhibitor selumetinib

MEK inhibitor, Selumetinib (Selleckchem, Houston, TX), was dissolved in 0.5% polymethyl cellulose (Sigma, USA). A volume of 250 µl of control vehicle or selumetinib (150 mg/kg of mouse body weight) was administered to each mouse by oral gavage at 6 h prior to 5-ALA injection.

3.3.2. Administration of 5-ALA *in vivo*

Athymic nude mice were injected intraperitoneally (i.p) with 5-ALA (200 mg/ kg BW) in sterile saline (0.85% NaCl) (Hospira, Canada) and kept in the dark for 2 h before light irradiation.

3.4. *In vitro* protoporphyrin IX (PpIX) measurements

The cells (5×10^4/well in 500 µl DMEM) were plated in a 24-well plate and incubated for 24 h to attain cell confluency of 75% - 80%. The medium was replaced with media containing U0126 or DMSO and then incubated for 20 h. After the incubation, they were treated with different concentrations of 5-ALA (0.2 mM, 1 mM, or 2 mM) for 4 h and then lysed with 100 µl of

radioimmunoprecipitation assay (RIPA) buffer (PBS pH 7.4, NP-40 1% (Sigma, USA), 0.1% sodium dodecyl sulfate (SDS) (Bio-Rad, Canada), 0.5% sodium deoxycholate (Sigma, USA). Cell lysates were diluted in PBS (190 μl of PBS and 5 μl cell lysate), and PpIX fluorescence was measured using Biotek Synergy MX fluorescent plate reader with a 405 nm excitation and 635 nm emission filter.

3.5. *In vitro* photodynamic therapy (PDT)

The cells (5×10^3 /well in 100 μl DMEM) were plated in a 96-well plate and incubated for 24 h to attain cell confluency of 75% - 80%. The medium was replaced with media supplemented with U0126 or DMSO and then incubated for 20 h. After the incubation, they were treated with different concentrations of 5-ALA (0.2 mM, 1 mM, or 2 mM) for 4 h in the dark. The culture medium was replaced with fresh medium, and the plates were irradiated with a 625 nm laser for 3 mins using a Theralase Modular Light source (TLC-3000A, Canada) (light density of 150 mW/cm^2 for 3 min, total energy of 27 J/cm^2).

3.6. Measurement of cell viability

At 24 h after PDT, a colorimetric cell viability kit (CCVK) (PromoCell, Canada) was used to measure cell viability. A volume of 10 μl of the reagent was added to each well (100 μl). They were incubated for 45 mins in the dark, and the absorbance was measured at 450 nm using a plate reader (Biotek, Vermont, USA). This assay uses tetrazolium salt WST-8, which is reduced by cellular dehydrogenase and formed an orange formazan product. The amount of this finished product is proportional to the number of live cells.

3.7. Animal studies

3.7.1. Mouse strains and housing

Eight-week-old athymic nude mice were obtained from Charles River Laboratories (strain 490, Homozygous, Crl:NU(NCr)-Foxn1nu), (Montreal) and housed in isolated ventilated caging units within the pathogen-free barrier at the central animal care facility in the Health Sciences Center at Memorial University of Newfoundland. The animal care protocols were approved by the Institutional Animal Care Committee in accordance with the Canadian Council on Animal Care guidelines. Mice were fed with Laboratory Rodent Diet 5010 food (27.5 % protein, 13.5 % fat, 59 % carbohydrate) (OM Nutrition International, Richmond, IN) with sterile water *ad libitum* and were housed under a 12-hour light/dark cycle.

3.7.2. Tumor xenograft mouse model

Human colon cancer cells (DLD-1) were grown as a monolayer in a 10 cm culture dish. Cells were trypsinized and washed three times in PBS. 2×10^6 cells in 100 μl PBS were injected subcutaneously into the right hind flank of the athymic nude mice.

3.7.3. PDT with MEK inhibitor, selumetinib

A schematic of the animal experiment is shown in Fig 5. After the development of palpable tumors (4-5 mm in diameter), selumetinib (150 mg selumetinib/kg BW) or control vehicle was administered to the mice by oral gavage. At 6 h after selumetinib treatment, the mice received 5-ALA (200 mg/kg BW) by i.p injection. All animals were anesthetized during the light treatment using isoflurane. A laser (Omicron Laserage, Germany) with the frontal light distributor (MedLight, S.A, Switzerland) was used as the light source to conduct PDT (energy density of 40

J/cm^2). Animals were kept in their home cages and maintained in a dark environment for 24 h after the light treatment to avoid 5-ALA-induced photosensitivity.

3.7.4. Measurement of tumor size

Tumor sizes were recorded in two dimensions using a pair of calipers every day till the tumor diameter reached 15 mm in any one dimension when the mice were euthanized by CO_2 inhalation.

Fig 5: *In vivo* experimental design. Athymic nude mice bearing human colon DLD-1 tumors on the right flank were treated p.o. with Selumetinib (250 mg/kg) for 6 h and then i.p. with 5-ALA (200 mg/kg) for 2 h. The tumors were irradiated with a 635 nm laser for 5 minutes to deliver an energy of 40 J/cm^2. The tumor sizes and mouse survival were monitored every day. Mice with tumor size of 15 mm in diameter in any directions were sacrificed as they were considered to reach the endpoint.

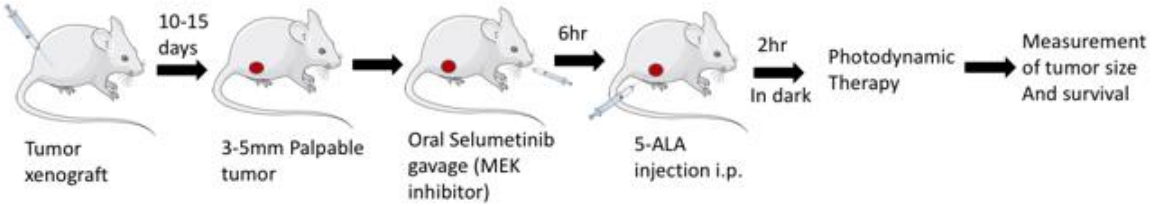
10-15
days
6hr
2hr
In dark
Photodynamic
Therapy
Measurement
of tumor size
And survival
Tumor
xenograft
3-5mm Palpable
tumor
Oral Selumetinib
gavage (MEK
inhibitor)
5-ALA
injection i.p.

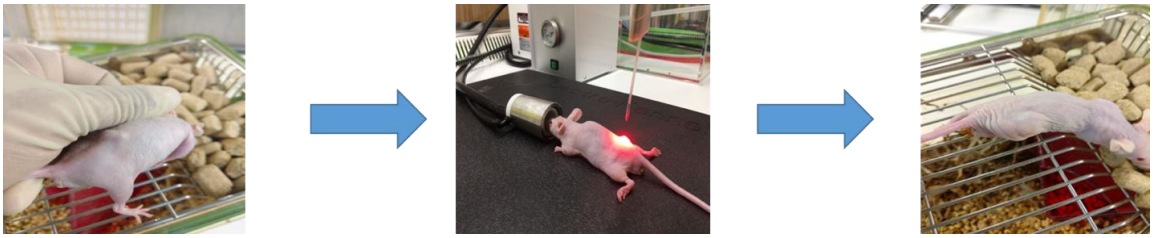

3.8. Statistical analysis

One-way ANOVA with Tukey's post-hoc test or Student's *t*-test was performed using GraphPad Prism 4.0 (GraphPad Software, La Jolla, CA, USA) to analyze the data. $p<0.01$ was considered significant for *in vitro* experiments and $p<0.05$ for *in vivo* experiments. Mouse survival was analyzed using the Kaplan-Meier log-rank test.

Chapter 4. Results

4.1. Sensitivity of different cancer cell lines to 5-ALA-PDT

To determine the sensitivity of different cancer cell lines to 5-ALA-PDT, we used seven cancer cell lines (U251, U118, DLD-1, H1299, Hs 578T, MDA-MB-231, and H460). The cells were plated in a 96-well plate, and, 24 h later, treated with different concentrations of 5-ALA (0.2 mM, 1 mM, or 5 mM) for 4 h in the dark and then irradiated at 625 nm red laser for 3 min using a Theralase Modular Light source (TLC-3000A, Canada). Cell viability was measured at 24 h after 5-ALA-PDT using a colorimetric cell viability kit (PromoCell, Canada). A cell line was deemed sensitive or not sensitive to the treatment based on the 24 h post-treatment-cell viability. A decrease in cell viability was perceived as a direct effect of the treatment, and the cell line was considered sensitive to the treatment. Different cell lines showed different levels of sensitivities to 5-ALA-PDT (Fig 5). Based on their sensitivity to 5-ALA-PDT, the seven human cancer cell lines were classified into three groups – sensitive, moderately sensitive, and least sensitive. U118 and U251 were killed by 5-ALA-PDT at all the concentrations tested and were classified as sensitive cell lines. DLD-1, H1299, Hs 578T, and MDA-MB-231 were sensitive to 5-ALA-PDT at the higher concentrations of 5-ALA (1 and 5 mM), but not at the lowest concentration of 5-ALA (0.2 mM), so they were classified as moderately sensitive cell lines. H460 was resistant to 5-ALA-PDT at all concentrations tested; therefore, it was classified as the least sensitive cell line.

Fig 6. Different cell lines have different sensitivities to 5-ALA-PDT. Human glioma (U-118, U-251), colon cancer (DLD-1), breast cancer (Hs 578T, MDA-MB-231), and lung cancer (H-1299, H460) cell lines were treated with 0, 0.2, 1, or 5 mM 5-ALA for 4 h in the dark before PDT irradiation with 635 nm light for 100 sec (27 J/cm^2). At 20 h after 5-ALA-PDT, cell viability was determined using a colorimetric cell viability kit. Data are expressed as the mean ± SD of fold changes in cell viability from 3 independent experiments compared to the control untreated cells. Statistical analysis was carried out using two-way ANOVA, with Turkey's post-hoc analysis. *$p<0.01$.

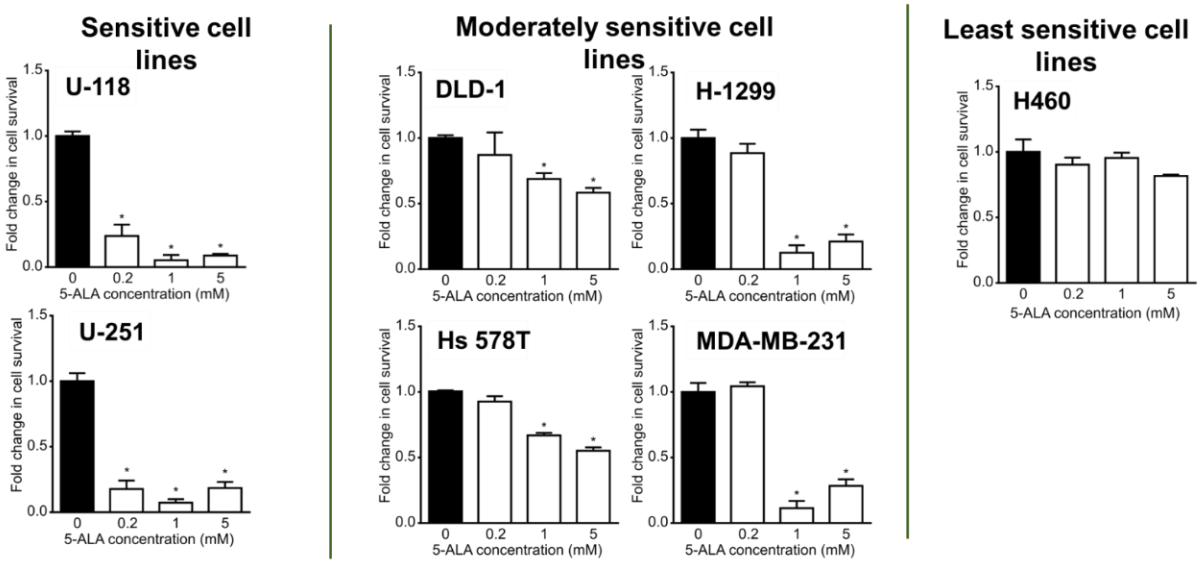
Sensitive cell lines
U-118
U-251
Moderately sensitive cell lines
DLD-1
H-1299
Hs 578T
MDA-MB-231
Least sensitive cell lines
H460
Fold change in cell survival
5-ALA concentration (mM)
0
0.2
1
5
0.0
0.5
1.0
1.5

4.2. MEK inhibition increased PpIX accumulation in moderately sensitive cell lines

Previously our laboratory demonstrated that MEK inhibition increases PpIX accumulation by inhibiting PpIX efflux and conversion to heme (Yoshioka *et al*., 2018). As sufficient PpIX accumulation is essential for effective 5-ALA-PDT, I hypothesized that MEK activation underlies the different sensitivities of human cancer cells to 5-ALA-PDT. To test this, I sought to determine whether MEK inhibition increases PpIX accumulation and 5-ALA-PDT efficacy in the moderately and least sensitive cell lines (Fig 6). Moderately sensitive cells (DLD-1 and Hs 578T) were treated with MEK inhibitor, U0126 (20 μM), or DMSO (vehicle control), for 20 h and then with different concentrations of 5-ALA (0.2, 1 or 5 mM) for 4 h in the dark. The cells were washed once with PBS and then lysed with 100 μl radioimmunoprecipitation assay (RIPA) buffer. PpIX fluorescence in the cell lysates was measured using a Biotek Synergy MX fluorescence plate reader with a 405 nm excitation and 635 nm emission filter. Both moderately sensitive cell lines showed significantly increased accumulation of PpIX. While DLD1 cells showed an increase in PpIX accumulation only when treated with 1 mM 5-ALA, Hs 578T cells showed significantly increased PpIX accumulation at both 1 mM and 5 mM 5-ALA, when pretreated with U0126.

Fig 7. MEK inhibition enhanced 5-ALA-induced PpIX accumulation. Human (A) colon cancer cells (DLD-1), and (B) breast cancer cells (Hs 578T) were treated with DMSO or MEK inhibitor (U0126) for 20 h, and then with 0.2, 1, or 5 mM 5-ALA and incubated in the dark for 4 h. The cells were lysed with RIPA buffer, and PpIX fluorescence in the lysates was measured using Biotek Synergy MX fluorescence plate reader with a 405 nm excitation and 635 nm emission filter. Data are expressed as the mean ± SD of fold changes in PpIX fluorescence from 3 independent experiments compared to the DMSO treated control. Statistical analysis was carried out using two-way ANOVA with Turkey's post-hoc test. *$p<0.01$.

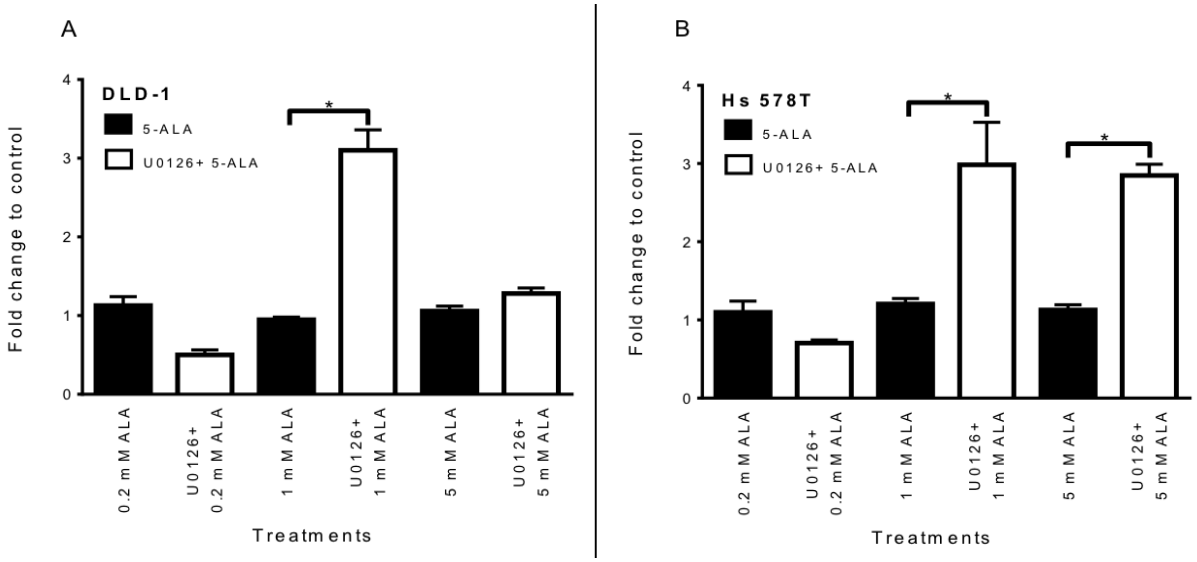
A
DLD-1
5-ALA
U0126+ 5-ALA
Fold change to control
0
1
2
3
4
*
0.2 m M ALA
U0126+ 0.2 m M ALA
1 m M ALA
U0126+ 1 m M ALA
5 m M ALA
U0126+ 5 m M ALA
Treatments
B
Hs 578T
5-ALA
U0126+ 5-ALA
Fold change to control
0
1
2
3
4
*
*
0.2 m M ALA
U0126+ 0.2 m M ALA
1 m M ALA
U0126+ 1 m M ALA
5 m M ALA
U0126+ 5 m M ALA
Treatments

4.3. MEK inhibitor increased sensitivity to 5-ALA-PDT in moderately sensitive cell lines

Next, I determined whether the increased accumulation of PpIX by MEK inhibition would improve the efficacy of 5-ALA-PDT in the moderately sensitive cell lines. DLD-1 and Hs 578T were treated with U0126 (20 μM) or DMSO for 20 h and then with different concentrations of 5-ALA (0.2 mM, 1 mM, or 5 mM) for 4 h. PDT was conducted by irradiating cells with a 625 nm red laser for 3 min using a Theralase Modular Light source (TLC-3000A, Canada). The efficacy of 5-ALA-PDT was determined by a colorimetric cell viability assay (PromoCell, Canada) at 24 h after treatment. Combined 5-ALA-PDT with U0126 showed significantly higher anti-cancer efficacies than 5-ALA-PDT only at the 5-ALA concentration of 1 and 5 mM in both DLD-1 and Hs 578T cells. Although combined treatment with U0126 and low ALA concentrations (0.2 – 1 mM) did not affect the sensitivity of the least sensitive cell line, H460, a slight but significant decrease in cell viability was observed at higher ALA concentrations (5, 7.5, and 10 mM). These results suggest that MEK activation in cancer cells reduces 5-ALA-mediated PpIX accumulation and, subsequently, their sensitivities to PDT.

Fig 8. MEK inhibition increases sensitivity to 5-ALA-PDT. Human (a) colon (DLD-1), (b) breast (Hs 578T), and (c) lung (H460) cancer cells were treated with DMSO or the MEK inhibitor (U0126) (20 μM) for 20 h, and then different concentrations of 5-ALA in the dark for 4 h. The cells were then subjected to PDT (635 nm light for 100 seconds: 27 J/cm^2). At 20 h after treatment, cell viability was assayed using a colorimetric cell viability kit. Data are expressed as the mean ± SD fold change in cell viability compared to the control untreated cells from 3 independent experiments. Statistical analysis was carried out using two-way ANOVA, with Turkey's post-hoc analysis. *$p<0.01$.

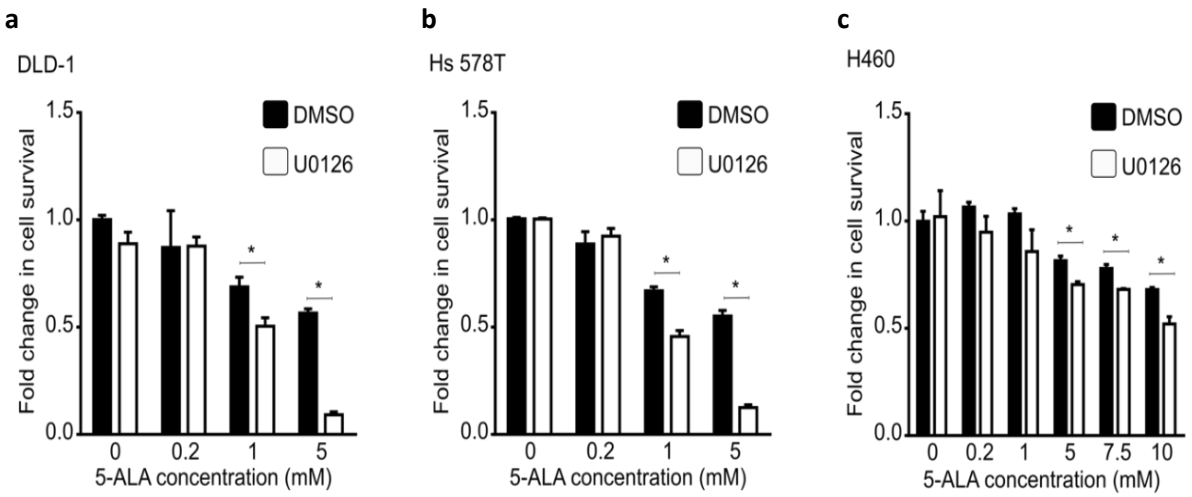
a
DLD-1
DMSO
U0126
Fold change in cell survival
1.5
1.0
0.5
0.0
0
0.2
1
5
5-ALA concentration (mM)
*
*
b
Hs 578T
DMSO
U0126
Fold change in cell survival
1.5
1.0
0.5
0.0
0
0.2
1
5
5-ALA concentration (mM)
*
*
c
H460
DMSO
U0126
Fold change in cell survival
1.5
1.0
0.5
0.0
0
0.2
1
5
7.5
10
5-ALA concentration (mM)
*
*
*

4.4. Combined 5-ALA-PDT treatment with MEK inhibitor reduced tumor volume and increased survival in athymic nude mice

To broaden our investigation, we next sought to determine whether MEK inhibition could promote the efficacy of 5-ALA-PDT *in vivo*. To answer this, I tested the efficacy of combined 5-ALA-PDT with the MEK inhibitor in nude mice bearing human tumor xenografts (Fig 8). For the *in vivo* experiments, I used the MEK inhibitor, selumetinib, which is being evaluated in Phase I and Phase II clinical trials for colorectal cancer, myeloma, biliary cancer, and hepatocellular carcinoma. (Bekaii-Saab *et al*., 2011; Muchir *et al*., 2012). Human colon DLD-1 cells were injected at the right hind flank of nude mice (2×10^6 cells in 100 μl PBS per mouse). When mice developed a palpable tumor (3-5 mm in diameter), they were grouped randomly into four groups – Control, selumetinib only, 5-ALA-PDT only, and combined 5-ALA-PDT with Selumetinib. Each group had nine mice. Selumetinib was administered orally (250 mg/kg BW), while vehicle control and 5-ALA-PDT only groups received vehicle (0.5% Propyl Methylcellulose in DW). The 5-ALA-PDT only and combined 5-ALA-PDT with Selumetinib groups were intraperitoneally injected with 5-ALA (200 mg/kg BW) at 6 h after inhibitor/vehicle treatment, followed by PDT at 2 h post-ALA administration. For PDT, a diode laser (Omicron Laserage, Germany) and a frontal light diffuser (MedLight, S.A, Switzerland) was used as the light source to deliver an energy density of 40 J/cm^2. The size of tumors was measured in two dimensions every day using a pair of calipers until 60 days after treatment or until the tumor size reached 15 mm in any dimension.

As tumors in the control group reached the maximum size within 12 days, all the mice were sacrificed (Fig 9). Selumetinib group showed slower but not significantly different tumor growth compared to the control group, and all mice reached the endpoint by 23 days after treatment. One

mouse in the selumetinib only group developed unrelated rashes, which was sacrificed before the tumor size reached the maximum level. While tumor growth of mice treated with 5-ALA-PDT was significantly slower compared to that of mice in the control group, all the mice were sacrificed within 23 days after treatment. Combined 5-ALA-PDT with Selumetinib significantly improved mice survival compared to control, selumetinib, or 5-ALA-PDT treatment. More importantly, four out of nine mice survived until the endpoint of the experiment (60 days after the treatment). Three of those mice were tumor-free, and the other had a very small tumor. In mice treated with the combined 5-ALA-PDT with Selumetinib, two mice were sacrificed before the tumors reached the maximum size due to the development of unrelated rashes.

These results demonstrate that MEK inhibitors can enhance the efficacy of *in vivo* ALA-PDT and prolong mice survival, suggesting that the combined treatment can be advantageous for cancer treatments in the clinical settings.

Fig 9. MEK inhibition enhanced 5-ALA-PDT efficacy *in vivo*. a) Growth of human colon DLD-1 tumors of mice treated with vehicle control (Control), Selumetinib (Selu), 5-ALA-PDT (ALA-PDT), or Selumetinib and 5-ALA-PDT (Selu-ALA-PDT). Each group had 9 mice, and each line represents the tumor sizes of an individual mouse. b) Kaplan-Meier survival curve showing the overall survival of mice in the four treatment groups. *$p<0.05$

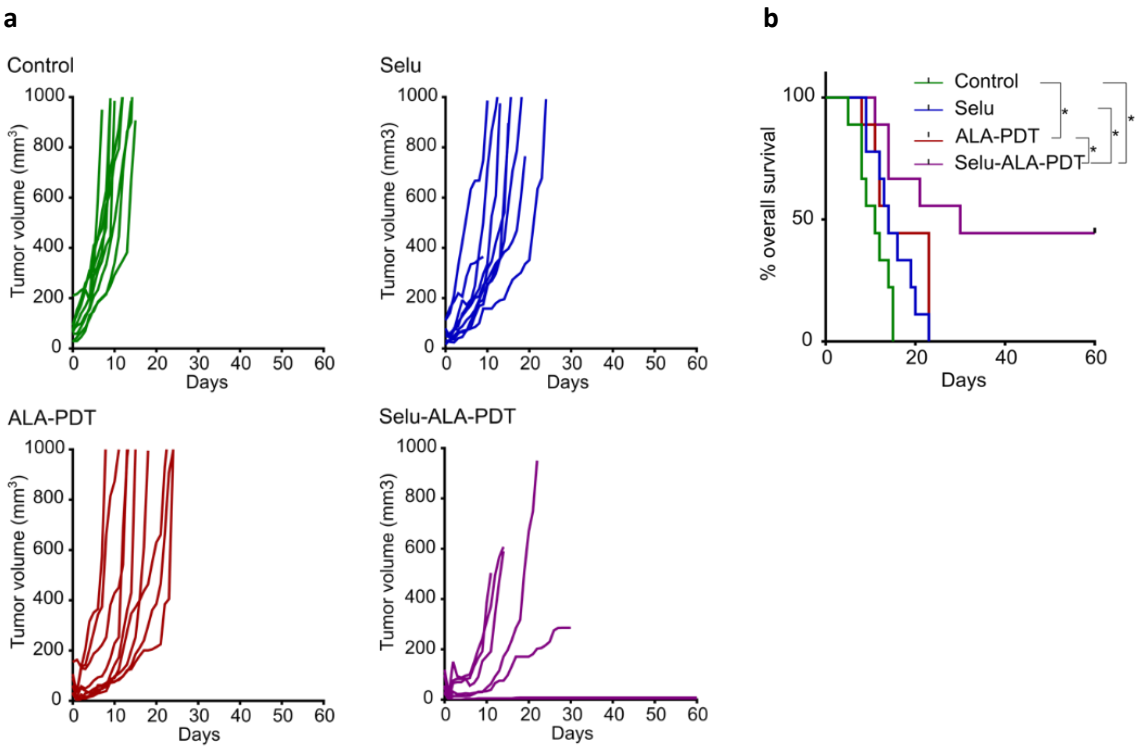
a
Control
Selu
ALA-PDT
Selu-ALA-PDT
Tumor volume (mm3)
Days
b
Control
Selu
ALA-PDT
Selu-ALA-PDT
% overall survival
Days

Chapter 5. Discussion

5.1. General discussion

Photodynamic Therapy (PDT), an alternative cancer therapy system, includes the administration of a PS and the production of reactive oxygen species triggered by light exposure, which leads to cancer cell death. The reactive oxygen species triggers rapid oxidization of biomolecules and cellular components, triggering several death triggers (Castano *et al*., 2004b, 2005a, 2005b). Previous studies have reported the initiation of apoptosis and necrosis after ROS mediated cellular oxidation (Agostinis *et al*., 2004; Coupienne *et al*., 2011; Quirk *et al*., 2015; Schreiber *et al*., 2002). It has also been reported that several cellular signaling pathways directly regulate the sensitivity of the cancer cells to ALA-PDT. Previously in Dr. Hirasawa Lab, we showed that the Ras/MEK signaling pathway regulates the accumulation of ALA-induced PpIX in cancer cells (Yoshioka *et al*., 2018). In this study, I evaluated whether the Ras/MEK signaling pathway also regulates ALA-PDT sensitivity in cancer cells.

In a cell, 5-aminolevulinic acid (5-ALA) can be metabolized into the fluorescent PS, protoporphyrin IX (PpIX). PpIX is further converted to heme by the enzyme ferrochelatase (FECH) or is effluxed out of the cells through the ABC binding cassette transporters such as ABCB1, ABCB6, and ABCG2 (Halani & Adamson, 2016; X. Yang *et al*., 2015). In cancer cells, exogenous treatment of 5-ALA leads to the accumulation of PpIX more efficiently than in normal cells due to an activated heme biosynthesis pathway and differences in the expression of porphyrin transporters, and mitochondrial activity (Castano *et al*., 2005a; Kammerer et al., 2011; X. Yang et al., 2015; Z. Zhang et al., 2015). Recently, our laboratory found that MEK inhibition increases PpIX accumulation in cancer cells. MEK, a downstream element of the Ras pathway, regulates the expression of ABCB1 and FECH activity. ABCB1 transports PpIX out of the

mitochondria and then out of the cell while FECH converts PpIX to heme (Kralova *et al*., 2017; Yoshioka *et al*., 2018). Therefore, the downregulation of ABCB1 expression and FECH activity results in the promotion of PpIX accumulation. Based on these findings, we were interested in determining whether increased PpIX accumulation in cancer cells by MEK inhibition can enhance 5-ALA-PDT efficacy as sufficient PpIX accumulation is essential for effective 5-ALA-PDT.

Based on these results, I sought to determine (objective 1) the sensitivity of different human cancer cell lines to 5-ALA-PDT and (objective 2) whether MEK inhibition increases 5-ALA-PDT efficacy *in vitro* and *in vivo*.

5.2. *In vitro* PDT and related mechanisms

To determine the sensitivity of cancer cells (objective 1), seven human cancer cell lines (U-118, U-251, DLD-1, Hs 578T, H1299, MDA-MB-231, and H460) were tested. Interestingly, we found that the cell lines showed different sensitivities to 5-ALA-PDT (Fig 5). Based on their sensitivity to 5-ALA-PDT, the cell lines were classified into three groups, sensitive, moderately sensitive, and least sensitive. Until now, the reason behind different sensitivities to 5-ALA-PDT of all these cell lines has not been clarified completely. A group of researchers found that inhibition of expressions of ABC transporters can lead to higher PpIX accumulation and enhance PDT effects in glioma cell lines (Zhao *et al*., 2013). Studies have shown that Caspase-dependent pathways (Chen *et al*., 2002), NF-κB transcription factors (Piette *et al*., 2003) (Matroule *et al*., 2001), MAPK signaling pathways (Assefa *et al*., 1999; Klotz *et al*., 1998), and membrane-mediated signal transductions (Agostinis *et al*., 2004; Dimitroff *et al*., 1999) might also be involved in

regulating PDT sensitivity. Particularly related to my research project, Liu J. *et al*. found that ALA-PDT activated MEK-ERK1/2 phosphorylation, and inhibition of this pathway increased the anti-cancer effects of ALA-PDT (Ge *et al*., 2016).

My results showed that different human cancer cell lines showed different sensitivities to 5-ALA-PDT *in vitro*. The glioma cell lines (U118 and U251) were very sensitive to 5-ALA-PDT as 5-ALA-PDT was effective even at the lowest concentration (0.2 mM) I tested, whereas the human lung cancer cell line (H460) was not sensitive to any concentrations of 5-ALA-PDT (0.2, 1 or 5 mM). DLD-1, HS 578T, MDA-MB-231, and H1299 were sensitive to 5-ALA-PDT at higher concentrations (1 mM and 5 mM) of 5-ALA, but not at the lowest concentration (0.2 mM). There have been very few publications demonstrating different sensitivity of human cancer cell lines to 5-ALA-PDT (Briel-Pump *et al*., 2018; Hadizadeh, 2014). As MEK inhibition restored cellular sensitivities to 5-ALA-PDT in the moderately and least sensitive cell lines (Fig 7), I believe that MEK activation modulates the cellular sensitivities. Nevertheless, the restoration of the sensitivities by MEK inhibition in the moderately and least sensitive cell lines was partial, suggesting that other cellular mechanisms are also involved in regulating cellular sensitivity to 5-ALA-PDT. These cellular mechanisms remain to be identified in the future. It is also of interest to determine whether activation levels of the Ras/MEK pathway in human cancer cell lines correlates with their sensitivities to 5-ALA-PDT. To test this, I would conduct western blotting analysis against phosphorylated ERKs, which are the downstream elements of MEK, on cell lysate obtained from the human cancer cell lines I used in this study. Moreover, I believe it is important to identify further downstream elements of the Ras/MEK/ERK pathway, which decreases cellular sensitivity to 5-ALA-PDT. The downstream elements currently identified are Mitogen-activated protein kinase (MAPK) interacting protein kinases 1 and 2 (MNK1-2),

Mitogen, and stress-activated protein kinase (MSK1-2), and ribosomal s6 kinase 1-4 (RSK1-4)(Whitmarsh, 2006). We would need to conduct experiments using chemical inhibitors, RNAi, and CRISPR knockdown of the targets to identify new downstream elements.

Several studies have explored the role of ABC transporters and the rate of PpIX efflux in deciding the sensitivity of the cells to ALA-PDT. It has been reported that PpIX efflux through ABCG2 is a key factor that regulates the sensitivity of cells to ALA-PDT (Barron *et al*., 2013). Inhibiting ABCG2 with an inhibitor, Ko-143, enhanced the efficacy of ALA-PDT in some cells. However, it was shown that ABCG2 inhibition could enhance PpIX accumulation even in normal cells leading to off-target effects of ALA-PDT (Barron *et al*., 2013; Yoshioka *et al*., 2018). Other studies have reported that the stage of the cell cycle and the degree of differentiation affects PDT sensitivity (Rollakanti *et al*., 2015; Wyld *et al*., 1998). It was shown that cells in the G_1 phase showed lower PpIX accumulation than those in the S or G_2 phases (Wyld *et al*., 1998). Furthermore, treatment with a differentiation-inducing agent such as Vitamin D enhanced ALA-PDT efficacy (S. Anand *et al*., 2013; Sanjay Anand *et al*., 2012; Rollakanti *et al*., 2015). This suggests that the differential sensitivity of the cell lines observed in the current study may be attributed to different factors. It is possible that the sensitive cell lines have a higher rate of PpIX metabolism, which promotes PpIX accumulation at a faster rate compared to the moderately sensitive cells and the least sensitive cells. Conversely, the least sensitive cell line might have a lower accumulation of PpIX. Further studies are required to identify the underlying mechanisms that regulate ALA-PDT sensitivity in different cell lines.

A previous study had reported that Ras-transformed breast cancer cells showed an increased accumulation of PpIX but had a lower sensitivity to ALA-PDT (Rodriguez *et al*., 2007). However, in our lab, we observed that treatment with a MEK inhibitor increased PpIX

accumulation in the sensitive and moderately sensitive cell lines (Fig. 7), suggesting that the activation of the Ras/MEK pathway reduced PpIX accumulation in cancer cells. It is possible that other Ras downstream elements might increase PpIX accumulation, while the Ras/MEK pathway has the opposite effect. However, further studies are required to clarify the role of the Ras signaling cascade in regulating PpIX accumulation.

To determine whether oncogenic Ras/MEK underlies cancer cell sensitivity to 5-ALA-PDT. To answer this question, DLD-1 and Hs 578T, which were classified as moderately sensitive cell lines, were chosen. Confirming the results from our previous study (Yoshioka *et al*., 2018), I found that MEK inhibition with U0126 increased PpIX accumulation in DLD-1 after 1 mM 5-ALA treatment and in Hs 578T after 1 mM and 5 mM 5-ALA treatments by almost 3 folds (Fig 6).

To test objective 2, I first determined whether MEK inhibition could increase the sensitivity to 5-ALA-PDT in the moderately sensitive cell lines. I found that combined 5-ALA-PDT with U0126 significantly decreased cell viability in DLD-1 and Hs 578T cells compared to 5-ALA-PDT only. To extend my study, I also determined whether MEK inhibition restores the 5-ALA-PDT sensitivity of the least sensitive cell line H460. As no visible changes in the sensitivity were observed in H460 cells after 5-ALA-PDT at 5-ALA concentrations of 0.2, 1, and 5 mM, I increased the 5-ALA concentrations up to 10 mM and found that H460 cells showed a significant decrease in cell viability after PDT. These results demonstrate that MEK activation underlies 5-ALA-PDT sensitivity in cancer cells. However, it should be noted that there may be other cellular mechanisms involved, as MEK inhibition did not completely restore 5-ALA-PDT sensitivity in the moderately and least sensitive cell lines (Fig 7).

5.3. *In vivo* PDT

Next, we determined whether MEK inhibition increases 5-ALA-PDT efficacy *in vivo* using a human colon cancer xenograft model. We observed slower tumor growth, a significant decrease in the tumor size, and higher survival rates in combined 5-ALA-PDT with Selumetinib compared to treatment with vehicle control, selumetinib only, or 5-ALA-PDT only. Particularly, 4 out of 9 mice in the combined treatment group survived until the end of the experiment (60 days), and 3 of them were tumor-free. Our *in vivo* results are in line with the *in vitro* data and support the hypothesis that the Ras/MEK signaling pathway regulates the sensitivity of cancers to 5-ALA-PDT.

To conclude, MEK inhibitors are excellent partners of 5-ALA-PDT to promote its efficacy *in vivo*. These results need to be further confirmed using different animal models of cancer and preclinical trials in the future. It should be noted that one mouse in the selumetinib only group developed unrelated rashes and was sacrificed early. It is currently unknown how the rashes were caused. However, other than the rashes, I did not observe any other side effects caused by selumetinib or 5-ALA-PDT.

Overall, my study demonstrates that oncogenic Ras/MEK activation underlies cancer cell sensitivities to 5-ALA-PDT and that MEK inhibition promotes the efficacy of 5-ALA-PDT *in vitro* and *in vivo*.

5.4. MEK inhibitors

The Ras/MEK pathway regulates many cellular activities, including cell proliferation, differentiation, and survival (Chang & Karin, 2001). As mutations of the pathway are often

involved in cancer development, it has been considered as a therapeutic target. MEK inhibitors are widely studied and evaluated as a monotherapy or combination therapy for other cancer treatments. There are three MEK inhibitors (trametinib, cobimetinib, and binimetinib) that are approved by FDA and EMA until now (Cheng *et al*., 2017; Research, 2018). Patients treated with MEK inhibitors sometimes develop mild side effects such as rashes, peripheral edema, diarrhea, and fatigue (Welsh & Corrie, 2015). MEK inhibitor U0126, which is used in this study, is developed for *in vitro* and *in vivo* animal studies. Selumetinib is highly competitive for MEK1/2 and is currently evaluated at Phase I and II clinical trials in humans. As the safety and efficacy of MEK inhibitors have been tested in clinical trials and other cancer therapeutic approaches, I believe that our results have a direct and immediate impact on improving 5-ALA-PDT efficacy in clinical settings. To further support moving our research toward clinical studies, it may be essential to confirm our results using the MEK inhibitors (trametinib, cobimetinib, and binimetinib) that have been approved by the FDA. It is also necessary to confirm the efficacy of combined 5-ALA-PDT with a MEK inhibitor in other animal models of cancer such as different types of human cancer cells, metastases model, and mice with human primary tumor xenograft.

Chapter 6. Conclusion and Future Directions

6.1. Conclusion

Various human cancer cells exhibit different sensitivity to 5-ALA-PDT. Oncogenic activation of the Ras/MEK pathway decreases cancer cell sensitivity to 5-ALA-PDT. MEK inhibition increased the 5-ALA-PDT sensitivities *in vitro* and *in vivo*.

6.2. Identification of other mechanisms regulating the sensitivity to 5-ALA-PDT in various cancer cell lines

We demonstrated that all seven cancer cell lines that were tested have different sensitivities to 5-ALA-PDT. As MEK inhibition restores the cellular sensitivity to 5-ALA-PDT of moderately and least sensitive cell lines, I concluded that Ras/MEK activation decreases the 5-ALA-PDT sensitivity. As MEK inhibition, however, did not induce complete restoration, I believe that there are other cellular mechanisms, such as regulation by Ras downstream pathways other than MEK, that regulate 5-ALA-PDT sensitivity. This needs to be addressed in future studies.

6.3. Determine whether other MEK inhibitors have similar effects on 5-ALA-PDT

MEK inhibitors U0126 and Selumetinib increased 5-ALA-PDT efficacy *in vitro* and *in vivo*, respectively. To confirm these results, we need to use different MEK inhibitors, particularly the ones approved by the FDA, such as trametinib, cobimetinib, and binimetinib, and determine whether they have a similar promotion of 5-ALA-PDT efficacy to U0126 and Selumetinib.

6.4. Determine whether combined 5-ALA-PDT with a MEK inhibitor is effective in different animal models of cancer.

The efficacy of the combined therapy was well documented in a human colon cancer xenograft model in this study. Nevertheless, it remains to be determined whether the combined therapy is effective in other animal models of cancer, such as human cancer xenograft with other type cancer cell lines, cancer metastasis models, and patient-derived xenograft (PDX) models.

Bibliography

Agostinis, P., Berg, K., Cengel, K. A., Foster, T. H., Girotti, A. W., Gollnick, S. O., Hahn, S. M., Hamblin, M. R., Juzeniene, A., Kessel, D., Korbelik, M., Moan, J., Mroz, P., Nowis, D., Piette, J., Wilson, B. C., & Golab, J. (2011). Photodynamic therapy of cancer: an update. *CA: A Cancer Journal for Clinicians*, *61*(4), 250–281. https://doi.org/10.3322/caac.20114

Agostinis, P., Buytaert, E., Breyssens, H., & Hendrickx, N. (2004). Regulatory pathways in photodynamic therapy induced apoptosis. *Photochemistry and Photobiological Sciences 3*(8), 721–9, https://doi.org/10.1039/b315237e

Anand, S., Hasan, T., & Maytin, E. (2013). Mechanism of Differentiation-Enhanced photodynamic therapy for cancer: upregulation of coproporphyrinogen oxidase by C/EBP transcription factors. *Molecular Cancer Therapeutics*, *12*(8), 1638–1650. https://doi.org/10.1158/1535-7163.MCT-13-0047

Anand, Sanjay, Ortel, B. J., Pereira, S. P., Hasan, T., & Maytin, E. V. (2012). Biomodulatory approaches to photodynamic therapy for solid tumors. *Cancer Letters*, *326*(1), 8–16. https://doi.org/10.1016/j.canlet.2012.07.026

Assefa, Z., Vantieghem, A., Declercq, W., Vandenabeele, P., Vandenheede, J. R., Merlevede, W., de Witte, P., & Agostinis, P. (1999). The activation of the c-Jun N-terminal kinase and p38 mitogen-activated protein kinase signaling pathways protects HeLa cells from apoptosis following photodynamic therapy with hypericin. *The Journal of Biological Chemistry*, *274*(13), 8788–8796. https://doi.org/10.1074/JBC.274.13.8788

Atkins, S., & He, F. (2019). Chemotherapy and beyond: Infections in the era of old and new treatments for hematologic malignancies. In *Infectious Disease Clinics of North America*

(Vol. 33, Issue 2, pp. 289–309). W.B. Saunders. https://doi.org/10.1016/j.idc.2019.01.001

Barron, G. A., Moseley, H., & Woods, J. A. (2013). Differential sensitivity in cell lines to photodynamic therapy in combination with ABCG2 inhibition. *Journal of Photochemistry and Photobiology B: Biology*, *126*, 87–96. https://doi.org/10.1016/j.jphotobiol.2013.07.003

Bekaii-Saab, T., Phelps, M. A., Li, X., Saji, M., Goff, L., Kauh, J. S. W., O'Neil, B. H., Balsom, S., Balint, C., Liersemann, R., Vasko, V. V, Bloomston, M., Marsh, W., Doyle, L. A., Ellison, G., Grever, M., Ringel, M. D., & Villalona-Calero, M. A. (2011). Multi-institutional phase II study of selumetinib in patients with metastatic biliary cancers. *Journal of Clinical Oncology : Official Journal of the American Society of Clinical Oncology*, *29*(17), 2357–2363. https://doi.org/10.1200/JCO.2010.33.9473

Briel-Pump, A., Beez, T., Ebbert, L., Remke, M., Weinhold, S., Sabel, M. C., & Sorg, R. V. (2018). Accumulation of protoporphyrin IX in medulloblastoma cell lines and sensitivity to subsequent photodynamic treatment. *Journal of Photochemistry and Photobiology B: Biology*, *189*(November), 298–305. https://doi.org/10.1016/j.jphotobiol.2018.11.002

Cancer. (2015). Retrieved September 30, 2020, from https://www.who.int/news-room/fact-sheets/detail/cancer

Carriere, A., Ray, H., Blenis, J., & Roux, P. P. (2008). The RSK factors of activating the Ras/MAPK signaling cascade. *Frontiers in Bioscience : A Journal and Virtual Library*, *13*(7), 4258–4275. https://doi.org/10.2741/3003

Casas, A., Battah, S., Di Venosa, G., Dobbin, P., Rodriguez, L., Fukuda, H., Batlle, A., & MacRobert, A. J. (2009). Sustained and efficient porphyrin generation *in vivo* using dendrimer conjugates of 5-ALA for photodynamic therapy. *Journal of Controlled Release*,

135(2), 136–143. https://doi.org/10.1016/j.jconrel.2009.01.002

Castano, A. P., Demidova, T. N., & Hamblin, M. (2004a). Mechanisms in photodynamic therapy: part one. *Photodiagnosis Photodyn Ther*, *1*(4), 279–293. https://doi.org/10.1016/S1572-1000(05)00007-4

Castano, A. P., Demidova, T. N., & Hamblin, M. R. (2005a). Mechanisms in photodynamic therapy: part two-cellular signaling, cell metabolism and modes of cell death. *Photodiagnosis and Photodynamic Therapy*, *2*(1), 1–23. https://doi.org/10.1016/S1572-1000(05)00030-X

Castano, A. P., Demidova, T. N., & Hamblin, M. R. (2005b). Mechanisms in photodynamic therapy: Part three - Photosensitizer pharmacokinetics, biodistribution, tumor localization and modes of tumor destruction. *Photodiagnosis and Photodynamic Therapy*, *2*(2), 91–106. https://doi.org/10.1016/S1572-1000(05)00060-8

Chang, L., & Karin, M. (2001). Mammalian MAP kinase signalling cascades. *Nature*, *410*(6824), 37–40. https://doi.org/10.1038/35065000

Chelakkot, V. S., Som, J., Yoshioka, E., Rice, C. P., Rutihinda, S. G., & Hirasawa, K. (2019). Systemic MEK inhibition enhances the efficacy of 5-aminolevulinic acid-photodynamic therapy. *British Journal of Cancer*, *121*(9), 758–767. https://doi.org/10.1038/s41416-019-0586-3

Chen, B., Roskams, T., Xu, Y., Agostinis, P., & de Witte, P. A. M. (2002). Photodynamic therapy with hypericin induces vascular damage and apoptosis in the RIF-1 mouse tumor model. *International Journal of Cancer*, *98*(2), 284–290. https://doi.org/10.1002/ijc.10175

Cheng, Y., Tian, H., Cheng, Y., & Tian, H. (2017). Current Development Status of MEK

Inhibitors. *Molecules*, *22*(10), 1551. https://doi.org/10.3390/molecules22101551

Chow, C. R., Ebine, K., Hattaway, H. Z., Kumar, K., & Munshi, H. G. (2017). Cross talk between snail and mutant k-ras contributes to pancreatic cancer progression. In *Conquering RAS: From Biology to Cancer Therapy* (pp. 119–131). Elsevier Inc. https://doi.org/10.1016/B978-0-12-803505-4.00007-2

Coupienne, I., Fettweis, G., Rubio, N., Agostinis, P., & Piette, J. (2011). 5-ALA-PDT induces RIP3-dependent necrosis in glioblastoma. *Photochemical & Photobiological Sciences*, *10*(12), 1868–1878. https://doi.org/10.1039/c1pp05213f

Datta, A., Kim, H., Lal, M., McGee, L., Johnson, A., Moustafa, A. A., Jones, J. C., Mondal, D., Ferrer, M., & Abdel-Mageed, A. B. (2017). Manumycin A suppresses exosome biogenesis and secretion via targeted inhibition of Ras/Raf/ERK1/2 signaling and hnRNP H1 in castration-resistant prostate cancer cells. *Cancer Letters*, *408*, 73–81. https://doi.org/10.1016/j.canlet.2017.08.020

Dimitroff, C. J., Klohs, W., Sharma, A., Pera, P., Driscoll, D., Veith, J., Steinkampf, R., Schroeder, M., Klutchko, S., Sumlin, A., Henderson, B., Dougherty, T. J., & Bernacki, R. J. (1999). Anti-angiogenic activity of selected receptor tyrosine kinase inhibitors, PD166285 and PD173074: implications for combination treatment with photodynamic therapy. *Investigational New Drugs*, *17*(2), 121–135.

Eroglu, Z., Tawbi, H. A., Hu, J., Guan, M., Frankel, P. H., Ruel, N. H., Wilczynski, S., Christensen, S., Gandara, D. R., & Chow, W. A. (2015). A randomised phase II trial of selumetinib vs selumetinib plus temsirolimus for soft-tissue sarcomas. *British Journal of Cancer*, *112*(10), 1644–1651. https://doi.org/10.1038/bjc.2015.126

Friday, B. B., & Adjei, A. A. (2008). Advances in targeting the Ras/Raf/MEK/Erk mitogen-activated protein kinase cascade with MEK inhibitors for cancer therapy. *Clinical Cancer Research, 14*(2), 342–346. https://doi.org/10.1158/1078-0432.CCR-07-4790

Ge, X., Liu, J., Shi, Z., Jing, L., Yu, N., Zhang, X., Jiao, Y., Wang, Y., & Li, P. A. (2016). Inhibition of MAPK signaling pathways enhances cell death induced by 5-Aminolevulinic acid-photodynamic therapy in skin squamous carcinoma cells. *European Journal of Dermatology*, *26*(2), 164–172. https://doi.org/10.1684/ejd.2015.2725

Gerber, D. E. (2008). Targeted therapies: A new generation of cancer treatments. *Americal Family Physician, 77*(3), 311-9.

Hadizadeh, M. (2014). Synergistic cytotoxic effect of gold nanoparticles and 5-aminolevulinic acid-mediated photodynamic therapy against skin cancer cells. *Iran Journal of Medical Science 39*(5), 452-8.

Halani, S. H., & Adamson, D. C. (2016). Clinical utility of 5-aminolevulinic acid HCl to better visualize and more completely remove gliomas. *OncoTargets and Therapy*, *9*, 5629–5642. https://doi.org/10.2147/OTT.S97030

Hawkins, T. A., Cavodeassi, F., Erdélyi, F., Szabó, G., & Lele, Z. (2008). The small molecule Mek1/2 inhibitor U0126 disrupts the chordamesoderm to notochord transition in zebrafish. *BMC Developmental Biology*, *8*(1), 42. https://doi.org/10.1186/1471-213X-8-42

How immunotherapy is used to treat cancer. (2015). Retrieved September 30, 2020, from https://www.cancer.org/treatment/treatments-and-side-effects/treatment-types/immunotherapy/what-is-immunotherapy.html

How radiation therapy is used to treat cancer. (2018). Retrieved September 30, 2020, from

https://www.cancer.org/treatment/treatments-and-side-effects/treatment-types/radiation/basics.html

Huang, Z. (2005). A review of progress in clinical photodynamic therapy. In *Technology in Cancer Research and Treatment* (Vol. 4, Issue 3, pp. 283–293). https://doi.org/10.1177/153303460500400308

Immunotherapy for cancer. (2019). Retrieved September 30, 2020, from https://www.cancer.gov/about-cancer/treatment/types/immunotherapy

Ishizuka, M., Abe, F., Sano, Y., Takahashi, K., Inoue, K., Nakajima, M., Kohda, T., Komatsu, N., Ogura, S. I., & Tanaka, T. (2011). Novel development of 5-aminolevurinic acid (ALA) in cancer diagnoses and therapy. *International Immunopharmacology*, *11*(3), 358–365. https://doi.org/10.1016/j.intimp.2010.11.029

Jablonski diagram. (2020, May 25). Retrieved September 30, 2020, from https://en.wikipedia.org/wiki/Jablonski_diagram

Jabłoństski, A. (1933). Efficiency of anti-stokes fluorescence in dyes [6]. In *Nature* (Vol. 131, Issue 3319, pp. 839–840). Nature Publishing Group. https://doi.org/10.1038/131839b0

Janda, E., Lehmann, K., Killisch, I., Jechlinger, M., Herzig, M., Downward, J., Beug, H., & Grünert, S. (2002). Ras and TGFβ cooperatively regulate epithelial cell plasticity and metastasis: Dissection of Ras signaling pathways. *Journal of Cell Biology*, *156*(2), 299–313. https://doi.org/10.1083/jcb.200109037

Juzeniene, A., Peng, Q., & Moan, J. (2007). Milestones in the development of photodynamic therapy and fluorescence diagnosis. *Photochemical and Photobiological Sciences*, *6*(12), 1234–1245. https://doi.org/10.1039/b705461k

Kammerer, R., Buchner, A., Palluch, P., Pongratz, T., Oboukhovskij, K., Beyer, W., Johansson, A., Stepp, H., Baumgartner, R., & Zimmermann, W. (2011). Induction of immune mediators in glioma and prostate cancer cells by non-lethal photodynamic therapy. *PloS One*, *6*(6), e21834. https://doi.org/10.1371/journal.pone.0021834

Khan, A. Q., Kuttikrishnan, S., Siveen, K. S., Prabhu, K. S., Shanmugakonar, M., Al-Naemi, H. A., Haris, M., Dermime, S., & Uddin, S. (2019). RAS-mediated oncogenic signaling pathways in human malignancies. *Seminars in Cancer Biology*, *54*, 1–13. https://doi.org/10.1016/j.semcancer.2018.03.001

Khunger, A., Khunger, M., & Velcheti, V. (2018). Dabrafenib in combination with trametinib in the treatment of patients with BRAF V600-positive advanced or metastatic non-small cell lung cancer: clinical evidence and experience. In *Therapeutic Advances in Respiratory Disease* (Vol. 12, p. 175346661876761). SAGE Publications Ltd. https://doi.org/10.1177/1753466618767611

Kim, C. H., Chung, C. W., Choi, K. H., Yoo, J. J., Kim, D. H., Jeong, Y. Il, & Kang, D. H. (2011). Effect of 5-aminolevulinic acid-based photodynamic therapy via reactive oxygen species in human cholangiocarcinoma cells. *International Journal of Nanomedicine*, *6*, 1357–1363. https://doi.org/10.2147/ijn.s21395

Klepper, B. (2016). The gold standard for current cancer treatment. In *JAMA Internal Medicine* (Vol. 176, Issue 8, pp. 1060–1061). American Medical Association. https://doi.org/10.1001/jamainternmed.2016.2932

Klotz, L.-O., Fritsch, C., Briviba, K., Tsacmacidis, N., Schliess, F., & Sies2, H. (1998). Activation of JNK and p38 but not ERK MAP Kinases in Human Skin Cells by 5-

Aminolevulinate-Photodynamic Therapy. *Cancer Research, 58*(19), 4297-300

Kralova, J., Kolar, M., Kahle, M., Truksa, J., Lettlova, S., Balusikova, K., & Bartunek, P. (2017). Glycol porphyrin derivatives and temoporfin elicit resistance to photodynamic therapy by different mechanisms. *Scientific Reports*, *7*(March), 44497. https://doi.org/10.1038/srep44497

Krammer, B., & Verwanger, T. (2009). Photodynamic therapy with aminolevulinic acid or its methyl ester: Which one is superior? *Medical Laser Application*, *24*(4), 221–226. https://doi.org/10.1016/J.MLA.2009.07.002

Leblanc, V., Tocque, B., & Delumeau, I. (1998). Ras-GAP controls Rho-mediated cytoskeletal reorganization through its SH3 domain. *Molecular and Cellular Biology*, *18*(9), 5567–5578. https://doi.org/10.1128/mcb.18.9.5567

Li, G., Szewczuk, M. R., Raptis, L., Johnson, J. G., Weagle, G. E., Pottier, R. H., & Kennedy, J. C. (1999). Rodent fibroblast model for studies of response of malignant cells to exogenous 5-aminolevulinic acid. *British Journal of Cancer*, *80*(5–6), 676–684. https://doi.org/10.1038/sj.bjc.6690409

Liang, F., Ren, C., Wang, J., Wang, S., Yang, L., Han, X., Chen, Y., Tong, G., & Yang, G. (2019). The crosstalk between STAT3 and p53/RAS signaling controls cancer cell metastasis and cisplatin resistance via the Slug/MAPK/PI3K/AKT-mediated regulation of EMT and autophagy. *Oncogenesis*, *8*(10), 1–15. https://doi.org/10.1038/s41389-019-0165-8

Lu, R. M., Hwang, Y. C., Liu, I. J., Lee, C. C., Tsai, H. Z., Li, H. J., & Wu, H. C. (2020). Development of therapeutic antibodies for the treatment of diseases. *Journal of Biomedical Science*, *27*(1), 1–30. https://doi.org/10.1186/s12929-019-0592-z

Matroule, J.-Y., Carthy, C. M., Granville, D. J., Jolois, O., Hunt, D. W. C., & Piette, J. (2001). Mechanism of colon cancer cell apoptosis mediated by pyropheophorbide-a methylester photosensitization. *Oncogene*, *20*(30), 4070–4084. https://doi.org/10.1038/sj.onc.1204546

Menzies, A. M., & Long, G. V. (2014). Dabrafenib and trametinib, alone and in combination for BRAF-mutant metastatic melanoma. *Clinical Cancer Research*, *20*(8), 2035–2043. https://doi.org/10.1158/1078-0432.CCR-13-2054

Muchir, A., Reilly, S. A., Wu, W., Iwata, S., Homma, S., Bonne, G., & Worman, H. J. (2012). Treatment with selumetinib preserves cardiac function and improves survival in cardiomyopathy caused by mutation in the lamin A/C gene. *Cardiovascular Research*, *93*(2), 311–319. https://doi.org/10.1093/cvr/cvr301

O'Neil, B. H., Goff, L. W., Kauh, J. S. W., Strosberg, J. R., Bekaii-Saab, T. S., Lee, R. M., Kazi, A., Moore, D. T., Learoyd, M., Lush, R. M., Sebti, S. M., & Sullivan, D. M. (2011). Phase II study of the mitogen-activated protein kinase 1/2 inhibitor selumetinib in patients with advanced hepatocellular carcinoma. *Journal of Clinical Oncology*, *29*(17), 2350–2356. https://doi.org/10.1200/JCO.2010.33.9432

Piette, J., Volanti, C., Vantieghem, A., Matroule, J.-Y., Habraken, Y., & Agostinis, P. (2003). Cell death and growth arrest in response to photodynamic therapy with membrane-bound photosensitizers. *Biochemical Pharmacology*, *66*(8), 1651–1659. https://doi.org/10.1016/S0006-2952(03)00539-2

Pinedo, H. M., & Giaccone, G. (1997). Chemotherapy. *Lancet*, *349*(SUPPL.2). https://doi.org/10.1016/s0140-6736(97)90012-x

PubChem. (2020). Retrieved September 30, 2020, from https://pubchem.ncbi.nlm.nih.gov/

Quirk, B. J., Brandal, G., Donlon, S., Vera, J. C., Mang, T. S., Foy, A. B., Lew, S. M., Girotti, A. W., Jogal, S., LaViolette, P. S., Connelly, J. M., & Whelan, H. T. (2015). Photodynamic therapy (PDT) for malignant brain tumors - Where do we stand? *Photodiagnosis and Photodynamic Therapy*, *12*(3), 530–544. https://doi.org/10.1016/j.pdpdt.2015.04.009

Radiation Therapy for Cancer. (2019). Retrieved September 30, 2020, from https://www.cancer.gov/about-cancer/treatment/types/radiation-therapy

Raguz, S., & Yagüe, E. (2008). Resistance to chemotherapy: new treatments and novel insights into an old problem. *British Journal of Cancer*, *99*(3), 387–391. https://doi.org/10.1038/sj.bjc.6604510

Research, C. for D. E. and. (2018). FDA approves encorafenib and binimetinib in combination for unresectable or metastatic melanoma with BRAF mutations. *Case Medical Research*. https://doi.org/10.31525/fda1-ucm611981.htm

Robert, C., Grob, J. J., Stroyakovskiy, D., Karaszewska, B., Hauschild, A., Levchenko, E., Chiarion Sileni, V., Schachter, J., Garbe, C., Bondarenko, I., Gogas, H., Mandalá, M., Haanen, J. B. A. G., Lebbé, C., Mackiewicz, A., Rutkowski, P., Nathan, P. D., Ribas, A., Davies, M. A., … Long, G. V. (2019). Five-year outcomes with dabrafenib plus trametinib in metastatic melanoma. *New England Journal of Medicine*, *381*(7), 626–636. https://doi.org/10.1056/NEJMoa1904059

Rodriguez, L., Divenosa, G., Batlle, A., Macrobert, A., & Casas, A. (2007). Response to ALA-based PDT in an immortalised normal breast cell line and its counterpart transformed with the Ras oncogene. *Photochemical & Photobiological Sciences*, *6*(12), 1306–1310. https://doi.org/10.1039/b704235c

Rollakanti, K. R., Anand, S., & Maytin, E. V. (2015). Vitamin D enhances the efficacy of photodynamic therapy in a murine model of breast cancer. *Cancer Medicine*, *4*(5), 633–642. https://doi.org/10.1002/cam4.361

Sanlorenzo, M., Choudhry, A., Vujic, I., Posch, C., Chong, K., Johnston, K., Meier, M., Osella-Abate, S., Quaglino, P., Daud, A., Algazi, A., Rappersberger, K., & Ortiz-Urda, S. (2014). Comparative profile of cutaneous adverse events: BRAF/MEK inhibitor combination therapy versus BRAF monotherapy in melanoma. *Comparative Study, 71*(6), 1102-09. https://doi.org/10.1016/j.jaad.2014.09.002

Sansaloni-Pastor, S., Bouilloux, J., & Lange, N. (2019). The dark side: Photosensitizer prodrugs. *Pharmaceuticals, 12*(4). https://doi.org/10.3390/ph12040148

Santarpia, L., Lippman, S. M., & El-Naggar, A. K. (2012). Targeting the MAPK-RAS-RAF signaling pathway in cancer therapy. *Expert Opinion on Therapeutic Targets*, *16*(1), 103–119. https://doi.org/10.1517/14728222.2011.645805

Schreiber, S., Gross, S., Brandis, A., Harmelin, A., Rosenbach-Belkin, V., Scherz, A., & Salomon, Y. (2002). Local photodynamic therapy (PDT) of rat C6 glioma xenografts with Pd-bacteriopheophorbide leads to decreased metastases and increase of animal cure compared with surgery. *International Journal of Cancer*, *99*(2), 279–285. https://doi.org/10.1002/ijc.10299

Schubbert, S., Shannon, K., & Bollag, G. (2007). Hyperactive Ras in developmental disorders and cancer. *Nature Reviews. Cancer, 7*(4), 295–308. https://doi.org/10.1038/nrc2109

Scott, A. M., Allison, J. P., & Wolchok, J. D. (2012). Monoclonal antibodies in cancer therapy. *Cancer Immunology, 12*(14).

SEER cancer statistics review, 1975-2016. (2020). Retrieved September 30, 2020, from https://seer.cancer.gov/archive/csr/1975_2016/

Shields, J. M., Pruitt, K., McFall, A., Shaub, A., & Der, C. J. (2000). Understanding Ras:' it ain't over "til it's over". *Trends in Cell Biology*, *10*(4), 147–154. http://www.ncbi.nlm.nih.gov/pubmed/10740269

Siegel, R. L., Miller, K. D., & Jemal, A. (2018). Cancer statistics, 2018. *CA: A Cancer Journal for Clinicians*, *68*(1), 7-30. doi:10.3322/caac.21442

Stout, M. C., Asiimwe, E., Birkenstamm, J. R., Kim, S. Y., & Campbell, P. M. (2014). Analyzing Ras-associated cell proliferation signaling. *Methods in Molecular Biology*, *1170*, 393–409. https://doi.org/10.1007/978-1-4939-0888-2_21

Targeted Therapy for Cancer. (2019). Retrieved September 30, 2020, from https://www.cancer.gov/about-cancer/treatment/types/targeted-therapies

Trametinib. (2019). Retrieved September 30, 2020, from https://www.cancer.gov/about-cancer/treatment/drugs/trametinib

Van Erp, A. E. M., Versleijen-Jonkers, Y. M. H., Van Der Graaf, W. T. A., & Fleuren, E. D. G. (2018). Targeted therapy-based combination treatment in rhabdomyosarcoma. *Molecular Cancer Therapeutics*, *17*(7), 1365–1380. https://doi.org/10.1158/1535-7163.MCT-17-1131

Wan, M. T., & Lin, J. Y. (2014). Current evidence and applications of photodynamic therapy in dermatology. *Clinical, Cosmetic and Investigational Dermatology*, *7*, 145–163. https://doi.org/10.2147/CCID.S35334

Weidhaas, J. B., Eisenmann, D. M., Holub, J. M., & Nallur, S. V. (2006). A conserved

RAS/mitogen-activated protein kinase pathway regulates DNA damage-induced cell death postirradiation in radelegans. *Cancer Research*, *66*(21), 10434–10438. https://doi.org/10.1158/0008-5472.CAN-06-2182

Welsh, S. J., & Corrie, P. G. (2015). Management of BRAF and MEK inhibitor toxicities in patients with metastatic melanoma. *Therapeutic Advances in Medical Oncology*, *7*(2), 122–136. https://doi.org/10.1177/1758834014566428

Whitmarsh, A. J. (2007). Regulation of gene transcription by mitogen-activated protein kinase signaling pathways. *Biochimica Et Biophysica Acta (BBA) - Molecular Cell Research*, *1773*(8), 1285-1298. doi:10.1016/j.bbamcr.2006.11.011

Wu, P. K., & Park, J. I. (2015). MEK1/2 inhibitors: molecular activity and resistance mechanisms. *Seminars in Oncology*, *42*(6), 849–862. https://doi.org/10.1053/j.seminoncol.2015.09.023

Wyld, L., Smith, O., Lawry, J., Reed, M. W., & Brown, N. J. (1998). Cell cycle phase influences tumour cell sensitivity to aminolaevulinic acid-induced photodynamic therapy *in vitro*. *Br J Cancer*, *78*(1), 50–55. http://www.ncbi.nlm.nih.gov/pubmed/9662250

Xiang, S., Bai, W., Bepler, G., & Zhang, X. (2017). Activation of Ras by Post-Translational Modifications. In *Conquering RAS: From Biology to Cancer Therapy* (pp. 97–118). Elsevier Inc. https://doi.org/10.1016/B978-0-12-803505-4.00006-0

Yang, E. J., & Chang, J. H. (2011). PD98059 induces the apoptosis of human cervical cancer cells by regulating the expression of Bcl2 and ERK2. *Biomed. Science Letters*, *17*(4), 2255-7415s.

Yang, X., Palasuberniam, P., Kraus, D., & Chen, B. (2015). Aminolevulinic acid-based tumor

detection and therapy: molecular mechanisms and strategies for enhancement. *International Journal of Molecular Sciences*, *16*(10), 25865–25880. https://doi.org/10.3390/ijms161025865

Yang, X., Palasuberniam, P., Myers, K. A., Wang, C., & Chen, B. (2016). Her2 oncogene transformation enhances 5-aminolevulinic acid-mediated protoporphyrin IX production and photodynamic therapy response. *Oncotarget*, *7*(36), 57798–57810. https://doi.org/10.18632/oncotarget.11058

Yoshioka, E., Chelakkot, V. S., Licursi, M., Rutihinda, S. G., Som, J., Derwish, L., King, J. J., Pongnopparat, T., Mearow, K., Larijani, M., Dorward, A. M., & Hirasawa, K. (2018). Enhancement of cancer-specific protoporphyrin ix fluorescence by targeting oncogenic Ras/MEK pathway. *Theranostics*, *8*(8), 2134–2146. https://doi.org/10.7150/thno.22641

Zhang, X., Cheng, Q., Yin, H., & Yang, G. (2017). Regulation of autophagy and EMT by the interplay between p53 and RAS during cancer progression. *International Journal of Oncology*, *51*(1), 18–24. https://doi.org/10.3892/ijo.2017.4025

Zhang, Z., Wang, S., Xu, H., Wang, B., & Yao, C. (2015). Role of 5-aminolevulinic acid-conjugated gold nanoparticles for photodynamic therapy of cancer. *Journal of Biomedical Optics*, *20*(5), 51043. https://doi.org/10.1117/1.JBO.20.5.051043

Zhao, S. G., Chen, X. F., Wang, L. G., Yang, G., Han, D. Y., Teng, L., Yang, M. C., Wang, D. Y., Shi, C., Liu, Y. H., Zheng, B. J., Shi, C. Bin, Gao, X., & Rainov, N. G. (2013). Increased expression of ABCB6 enhances protoporphyrin IX accumulation and photodynamic effect in human glioma. *Annals of Surgical Oncology*, *20*(13), 4379–4388. https://doi.org/10.1245/s10434-011-2201-6